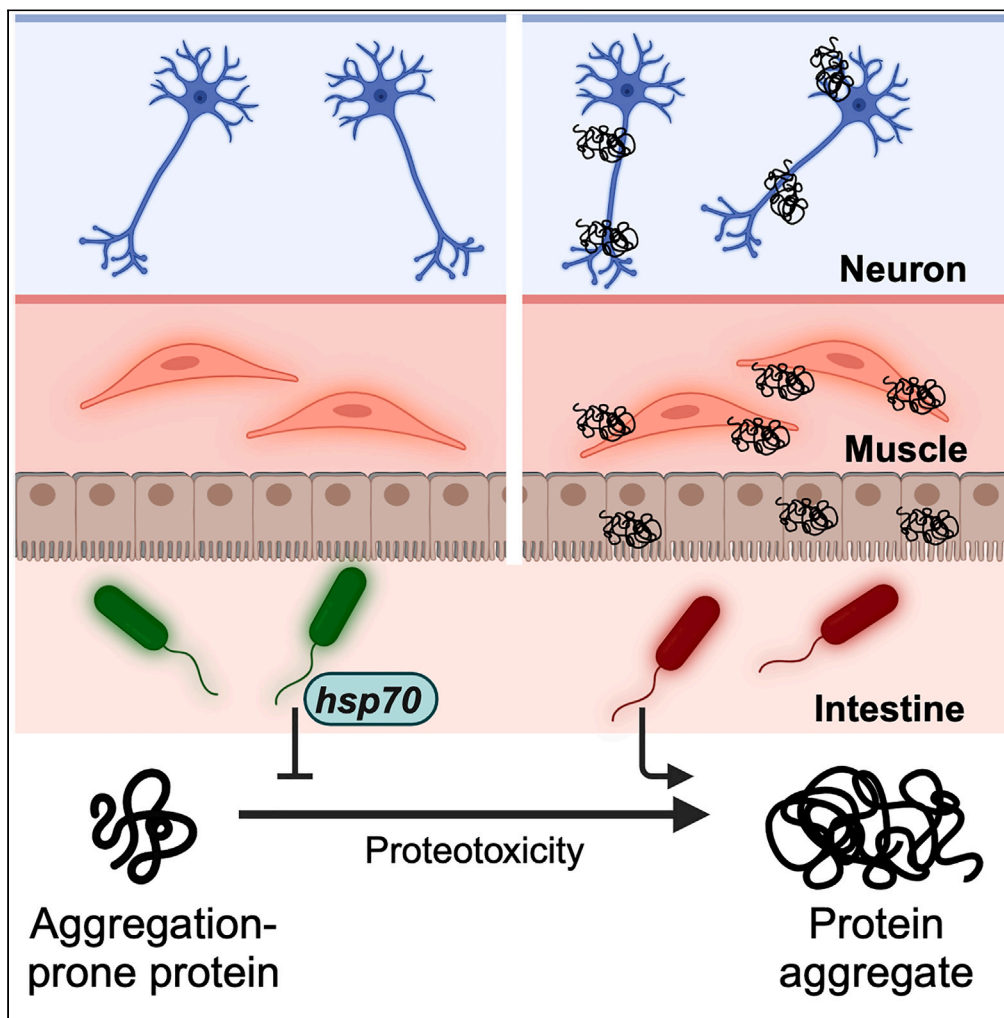


Article

Identification of proteotoxic and proteoprotective bacteria that non-specifically affect proteins associated with neurodegenerative diseases



Alyssa C. Walker,
Rohan Bhargava,
Michael J. Bucher,
Yoan M. Argote,
Amanda S. Brust,
Daniel M. Czyż

dczyz@ufl.edu

Highlights

Characterization of 229
bacterial isolates on host
protein stability

Bacteria affect the stability
of disease-associated
proteins

Proteoprotective
Prevotella corporis
activates the host heat
shock response

Gram-negative aerobes
induce broad
proteotoxicity in the host

Walker et al., iScience 27,
110828
September 20, 2024 © 2024
The Author(s). Published by
Elsevier Inc.
[https://doi.org/10.1016/
j.isci.2024.110828](https://doi.org/10.1016/j.isci.2024.110828)

Article

Identification of proteotoxic and proteoprotective bacteria that non-specifically affect proteins associated with neurodegenerative diseases

Alyssa C. Walker,¹ Rohan Bhargava,^{1,2} Michael J. Bucher,¹ Yoan M. Argote,¹ Amanda S. Brust,^{1,3} and Daniel M. Czyż^{1,4,*}

SUMMARY

There are no cures for neurodegenerative protein conformational diseases (PCDs), such as Alzheimer's disease (AD), Parkinson's disease (PD), and Huntington's disease (HD). Emerging evidence suggests the gut microbiota plays a role in their pathogenesis, though the influences of specific bacteria on disease-associated proteins remain elusive. Here, we reveal the effects of 229 human bacterial isolates on the aggregation and toxicity of A β ₁₋₄₂, α -synuclein, and polyglutamine tracts in *Caenorhabditis elegans* expressing these culprit proteins. Our findings demonstrate that bacterial effects on host protein aggregation are consistent across different culprit proteins, suggesting that microbes affect protein stability by modulating host proteostasis rather than selectively targeting disease-associated proteins. Furthermore, we found that feeding *C. elegans* proteoprotective *Prevotella corporis* activates the heat shock response, revealing an unexpected discovery of a microbial influence on host proteostasis. Insight into how individual bacteria affect PCD proteins could open new strategies for prevention and treatment by altering the abundance of microbes.

INTRODUCTION

Neurodegenerative protein conformational diseases (PCDs) are characterized by disturbances in proteostasis that result in the aggregation of disease-associated proteins, ultimately leading to tissue death.¹ Alzheimer's disease (AD), Parkinson's disease (PD), Huntington's disease (HD), and amyotrophic lateral sclerosis (ALS) are among the most prevalent neurodegenerative diseases, with AD recognized by the World Health Organization (WHO) as one of the leading causes of death worldwide.² However, despite the increasing prevalence of PCDs, their complex etiologies continue to obscure potential therapeutic targets. The sporadic onset and variable severity of neurodegenerative diseases, along with their idiopathic nature, suggest the role of a triggering factor in their onset and progression. Multiple factors have been associated with the pathogenicity of PCDs, including an expanding body of evidence that suggests the involvement of microbes, but primarily those within the human gut microbiota. The human gut microbiota is considered an "organ" due to its production of essential proteins and metabolites, including vitamins, hormones, and neurotransmitters.^{3,4} Hence, dysbiosis of the gut microbiota has been linked to various ailments, including neurodegenerative diseases.⁵

The complexity of the microbiome has made it challenging to determine the precise role of bacteria in the pathogenesis of neurodegenerative diseases. In addition, most of the evidence that associates bacteria with the occurrence of neurodegenerative diseases is based on correlation.⁶ Interestingly, correlational evidence does not demonstrate any selectivity between different neurodegenerative diseases, despite each disease featuring a unique, specific culprit protein species. For example, a lower abundance of *Prevotella* spp. has been observed in patients with different PCDs, including PD and ALS.⁷⁻¹⁵ Due to this lack of specificity, we hypothesized that bacteria could be affecting these diseases through the host proteostasis network—upstream of protein aggregate formation. This hypothesis is further supported by our previous study in which we identified gram-negative enteropathogens that significantly disrupt proteostasis across tissues in *Caenorhabditis elegans*.¹⁶ The utility of *C. elegans* as a model to study host-microbe interaction is strengthened by its unique ability to be colonized by a single bacterial strain. Such a feature simplifies the complexity of the microbiome, allowing us to study the effect of individual species on host proteostasis.

Here, we characterized the effect of 229 unique bacterial isolates from the Human Microbiome Project on the aggregation of disease-associated proteins in *C. elegans*. We used transgenic nematodes expressing A β ₁₋₄₂, α -synuclein, and polyglutamine (polyQ), proteins that adopt amyloid conformation and are associated with AD, PD, and HD, respectively, in which their toxic aggregation culminates in neurodegeneration.

¹Department of Microbiology and Cell Science, University of Florida, Gainesville, FL 32611, USA

²Present address: Feinberg School of Medicine, Northwestern University, Chicago, IL 60611, USA

³Present address: Department of Oncology, Albert Einstein College of Medicine, Bronx, NY 10461, USA

⁴Lead contact

*Correspondence: dczyz@ufl.edu

<https://doi.org/10.1016/j.isci.2024.110828>



Surprisingly, our results suggest that bacteria-mediated enhancement or suppression of host protein aggregation is not specific to any particular culprit protein. Instead, our data demonstrate that bacteria broadly affect the aggregation of metastable proteins present within the host proteome. Furthermore, we also observed that the proteostasis-modulating effects of intestinal bacteria reach distal tissues. Thus, our results indicate that bacteria influence host proteostasis, ultimately affecting the ability of both proximal and distal tissues to buffer protein folding. To date, the present study provides the most comprehensive characterization of the effect of individual constituents of the human microbiome on host proteostasis. Our findings reveal the bacterial contribution to the stability of not only proteins associated with AD, PD, and HD, but also endogenous host proteins, and may extrapolate to a broader range of metastable proteins implicated in various proteinopathies. Collectively, our results provide a framework for the development of microbiome-based risk factor assessments and disease management strategies.

RESULTS

Characterization of the human microbiome on host proteostasis

We obtained a comprehensive Human Microbiome Project collection of 229 unique bacterial isolates from Biodefense and Emerging Infections Research Resources Repository (BEI Resources) and assessed their effect on *C. elegans* proteostasis. The method used to conduct this experiment is illustrated in Figure 1. The collection encompasses isolates from a range of diverse phyla and a variety of anatomical sites (Figure 2). In our previous study, we used aggregation-prone polyQ tracts as a sensor of the protein folding environment to demonstrate that gram-negative pathogens disrupt host proteostasis.¹⁶ Among animals expressing intestine-, muscle-, and neuron-specific polyQ::YFP (yellow fluorescent protein), we previously found that proteostasis in the intestine was most robustly affected by the colonizing bacteria.¹⁶ As such, we performed our initial screen using the intestinal polyQ model (Figure 2). To eliminate the possibility that bacteria will affect *C. elegans* development, worms were grown to adulthood prior to being transferred to the bacterial strains of interest. PolyQ aggregation was assessed by fluorescent microscopy. To ensure the validity of our results, we also assessed polyQ aggregation by western blotting. Both quantitative methods yielded similar results, validating our approach.

Bacteria from the isolate collection exhibited a differential effect on *C. elegans* proteostasis as indicated by increases and decreases in polyQ aggregation compared to worms fed control *Escherichia coli* OP50 (Figure 2). Figure 2 summarizes the screen, revealing bacteria that most robustly affected host proteostasis. *Prevotella* was the only genus that consistently resulted in low polyQ aggregation across all 229 strains tested (Figure 2). Conversely, significant host proteotoxicity was observed in nematodes that were fed *Achromobacter xylosoxidans* and *Arcobacter butzleri*, as well as *Citrobacter*, *Escherichia*, *Klebsiella*, *Pseudomonas*, and *Ralstonia* spp. (Figure 2). A detailed list of all bacterial strains and their effect on polyQ aggregation is summarized in Table S1. Intriguingly, our data align with previous research linking the depletion or enrichment of these bacteria in patients with PCDs, which is further described in the discussion section of the present study. To our knowledge, this is the first-ever comprehensive screen that assessed the effect of human bacterial isolates on host proteostasis.

Prevotella spp. mitigate the proteotoxic aggregation of diverse culprit proteins

Out of the 229 strains tested, the *Prevotella* genus had the highest number of members that suppressed polyQ aggregation. We further retested 17 *Prevotella* spp. using the intestinal polyQ44 model. To increase the robustness of the response, we started feeding animals test bacteria immediately after hatching. Although we observed an enhanced suppression of aggregation for most retested strains, there were few isolates that did not significantly inhibit polyQ aggregation, likely due to the timing of feeding. Furthermore, as expected, feeding worms test bacteria beginning at the L1 larval stage affected development (Figure 3A, "Aggregates"). Out of all strains, *Prevotella buccae*, *Prevotella oris*, and *Prevotella corporis* significantly suppressed polyQ aggregation without causing any detectable developmental delay (Figure 3A, "Aggregates"). Therefore, we followed up with these three strains. Motility defects are associated with neurodegenerative PCDs. As such, we assessed whether the three *Prevotella* spp. alleviate aggregate-dependent motility defects caused by culprit proteins expressed in the intestine and distal tissues. We used our well-established and validated time-off-pick (TOP) assay that relies on *C. elegans* motility as a readout of proteotoxicity.^{16,17} Consistent with their suppression of polyQ aggregation, all three strains alleviated aggregate-dependent motility defects, with *P. corporis* having the strongest effect (Figure 3A, "Motility"). To determine whether the observed suppression is dependent on polyQ, we used N2 wild-type worms and a model expressing a shorter polyQ tract, polyQ33. The results revealed no effect on the N2 worms and a less robust suppression of the motility defect for polyQ33, indicating that *Prevotella* suppressed proteotoxicity. Given that dietary restriction enhances proteostasis and suppresses polyQ aggregation,¹⁸ we assessed pharyngeal pumping to determine whether the proteoprotective effect mediated by *P. corporis* could be the result of caloric restriction. Our results showed no significant difference in pharyngeal pumping between worms fed *E. coli* OP50 and those fed *P. corporis* (Figure S1), indicating that the observed proteoprotection is not caused by caloric restriction.

Because *Prevotella* spp. are anaerobic and may not thrive well in the ambient conditions in which *C. elegans* are cultured, we investigated whether dead bacteria retain their proteoprotective properties. To accomplish this, we fed worms paraformaldehyde (PFA)-killed bacteria and found that *P. corporis* still significantly suppressed polyQ aggregation relative to *E. coli* OP50 control (Figure S2), suggesting that live bacteria are not necessary to elicit protection.

To determine whether *Prevotella* also affects polyQ in distal tissues, we employed the neuronal and muscle models. Because worms expressing the neuronal polyQ do not exhibit quantifiable aggregates, we used the TOP assay as a proteotoxicity readout. Our results show that of the three strains, only *P. corporis* showed significant suppression of the motility defect in worms expressing neuronal polyQ40 (Figure 3B). Unexpectedly, *P. buccae*, *P. oris*, and *P. corporis* increased motility defects in worms expressing the neuronal empty vector control (polyQ0); the reason for this is unknown, but importantly does not diminish the observed beneficial effects of *Prevotella* on neuronal polyQ. In a manner

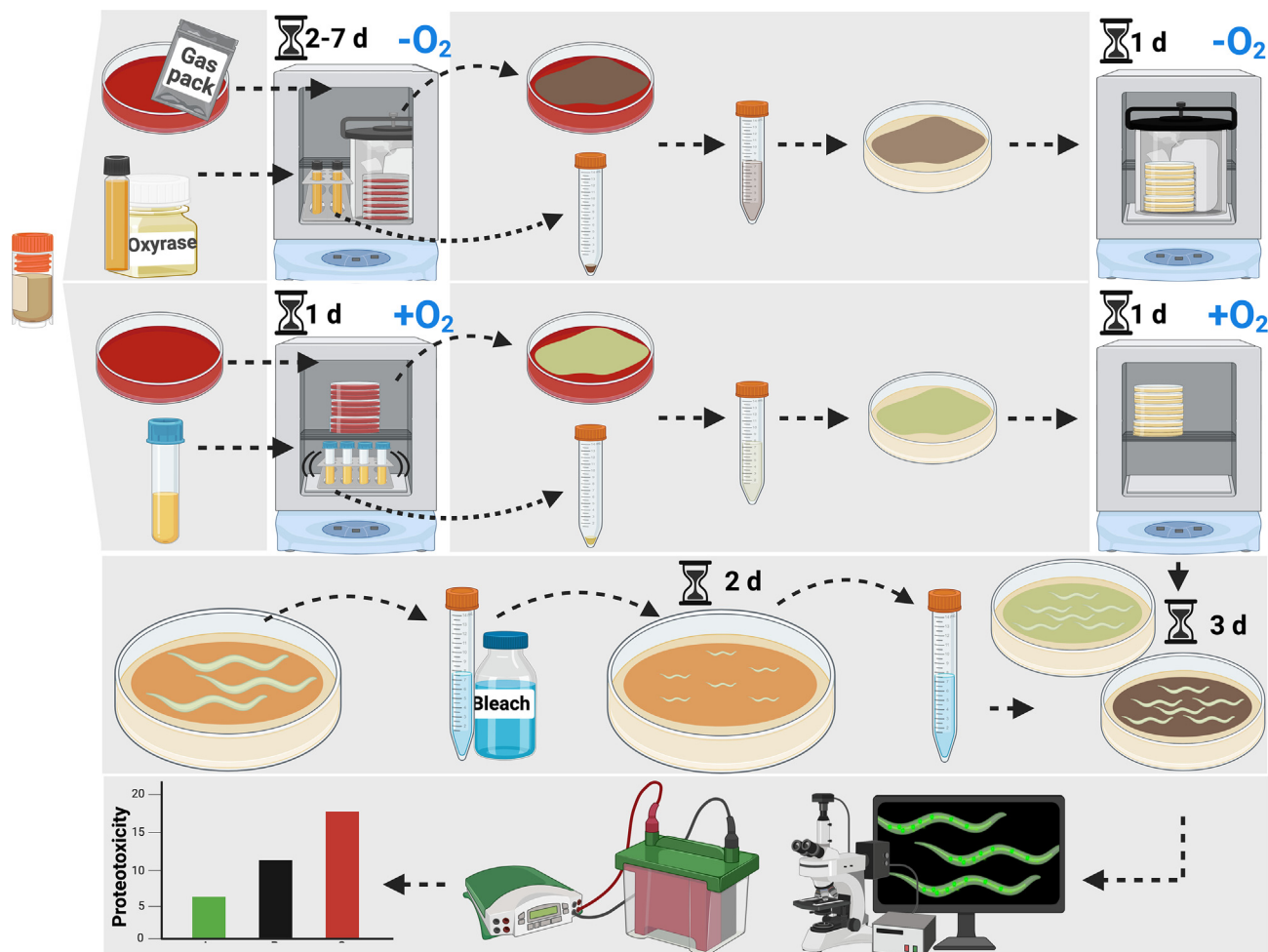


Figure 1. Schematic illustrating the method used to assess the effect of bacterial isolates on *C. elegans* proteotoxicity

Details can be found in [STAR methods](#). In brief, anaerobic bacteria were cultured on TSA-blood plates using anaerobic gas packs or in liquid broth supplemented with oxyrase for 2–7 days, while aerobic bacteria were cultured on TSA-blood plates or in liquid broth for one day. Cultured bacteria were transferred to nematode growth media (NGM) plates and incubated overnight with (for anaerobic bacteria) or without (aerobic bacteria) anaerobic gas packs. Worms were synchronized by the bleaching method and cultured on control *E. coli* OP50 until young adults (2 days), washed and transferred to NGM plates containing anaerobically or aerobically grown test bacteria, and cultured for an additional three days. Intestinal polyQ aggregates were quantified by manual counting and western blotting the insoluble fractions.

similar to the intestinal polyQ, we observed *Prevotella*-mediated suppression of aggregation and proteotoxicity in worms expressing muscle-specific polyQ (Figure 3C).

The association between the low abundance of gut *Prevotella* and diverse neurodegenerative PCDs suggests that the bacterial influence on these diseases is independent of the culprit protein species.^{8–14} As such, we hypothesized that bacteria might affect protein aggregation by modulating host proteostasis, and if this is the case, *Prevotella* spp. should enhance proteostasis in worms expressing various aggregation-prone proteins. To test the effect of *Prevotella* on other disease-associated proteins, we chose three muscle-specific models: one expressing A β _{1–42}, and two expressing α -synuclein.^{19–21} These culprit proteins are associated with Alzheimer’s and Parkinson’s diseases, respectively. Additionally, these models exhibit age-dependent proteotoxicity, which is consistent with the age-dependent progression of neurodegenerative diseases.^{16,22,23} To investigate progressive proteotoxicity in the A β _{1–42} and α -synuclein models,^{19–21} we assessed their motility between days three to five post-hatching (Figure S3). Nematodes expressing A β _{1–42} and α -synuclein had age-dependent motility defects that were markedly greater than those of the controls (Figure S3). We examined the effect of *P. buccae*, *P. oris*, and *P. corporis* on proteotoxicity associated with each of these three models. In a manner similar to the polyQ models, *P. buccae*, *P. oris*, and *P. corporis* reduced aggregate-dependent toxicity compared to wild-type control (Figure 3A), particularly with *P. corporis* having the strongest effect (Figures 3D and 3E). Bacteria that strongly enhance or suppress host proteostasis induce notable differences in the aggregation of A β _{1–42}, which parallels the extent of the motility defect (Figure S4). Both A β _{1–42} aggregation and the associated toxicity were suppressed by *P. corporis* and enhanced by *Pseudomonas aeruginosa* (Figure S4), a bacterium that strongly disrupted host proteostasis in our previous studies.^{16,24} Since all of our

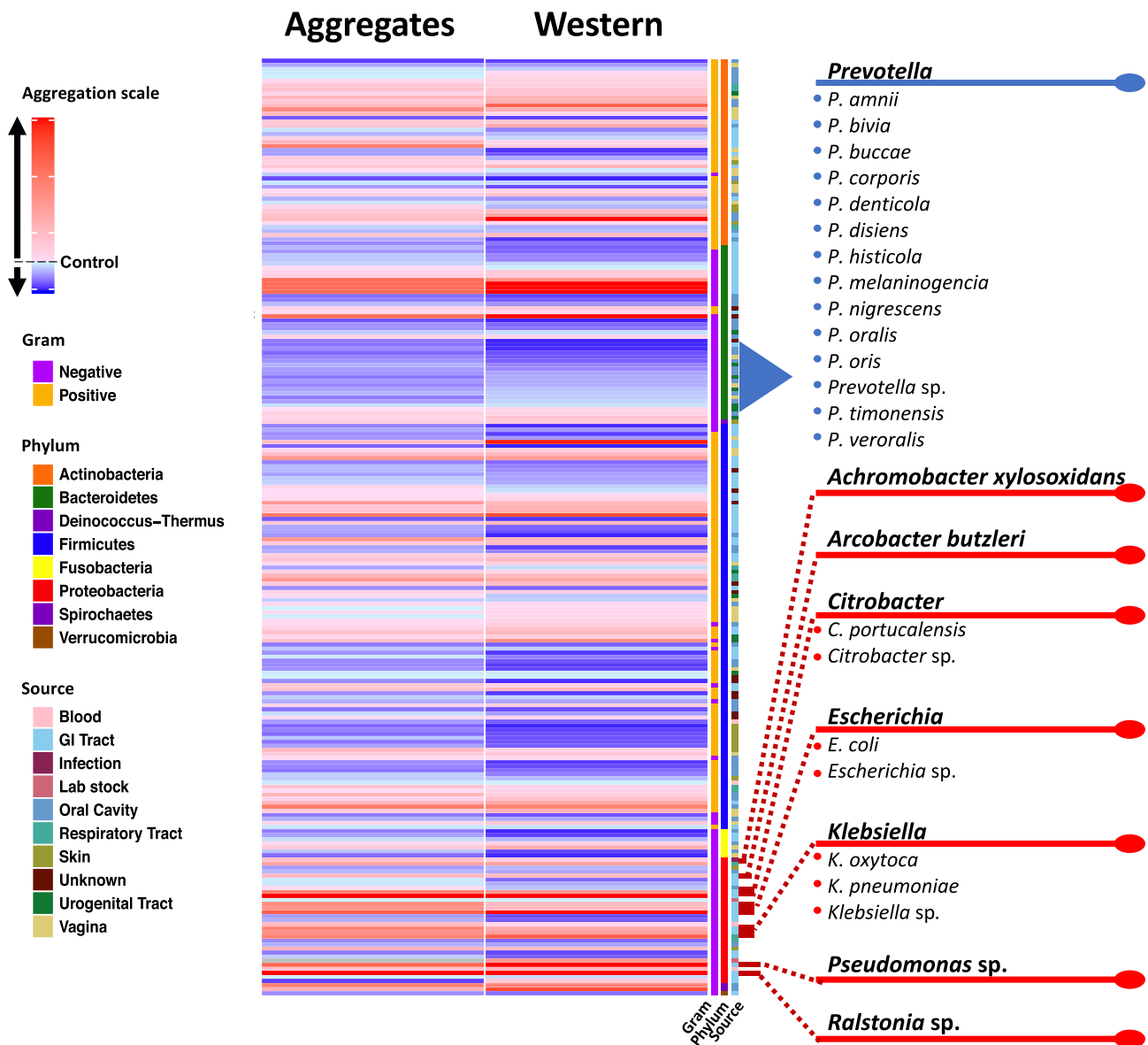


Figure 2. Heatmap summarizing the results of the screen that assessed the effect of human bacterial isolates on *C. elegans* intestinal polyQ aggregation PolyQ aggregation was quantified by microscopy (Aggregates column) and western blotting (Western column). Each of the 229 rows represents a single bacterial strain. Aggregation data are normalized to worms fed control *E. coli* OP50. The aggregation scale is color-coded from blue to red, where red indicates increasing polyQ aggregation relative to control. The characteristics (Gram, phylum, and source) of each bacterial isolate are included in the last three columns.

transgenic worms express exogenous proteins, we wanted to determine whether *Prevotella* can also provide protection against the misfolding of endogenous proteins. To accomplish this, we employed two strains that carry temperature-sensitive mutations in endogenous proteins: myosin heavy chain (UNC-54) that misfolds and leads to paralysis at the restrictive temperature (25°C),^{25,26} and DYN-1, featuring a modified GTPase domain that is highly expressed in motor neurons, resulting in loss of coordination at the restrictive temperature (25°C).²⁷ In agreement with the proteoprotective effect against misfolding and aggregation of exogenous proteins, *Prevotella* suppressed the temperature-dependent motility defect of both worm strains at the restrictive temperature, further supporting its proteoprotective role (Figure S5). Collectively, our findings suggest the broader potential of *Prevotella* in mitigating the pathogenesis of neurodegenerative diseases.

Proteotoxic bacteria enhance the aggregation and toxicity of PCD-associated proteins

To confirm the effect of the most robust proteotoxic strains identified in our original screen (Figure 2; Table S1), we assessed polyQ44 aggregation in animals fed gram-negative aerobes (Figure 4A, "Aggregates"). We concentrated on these specific bacteria because they did not

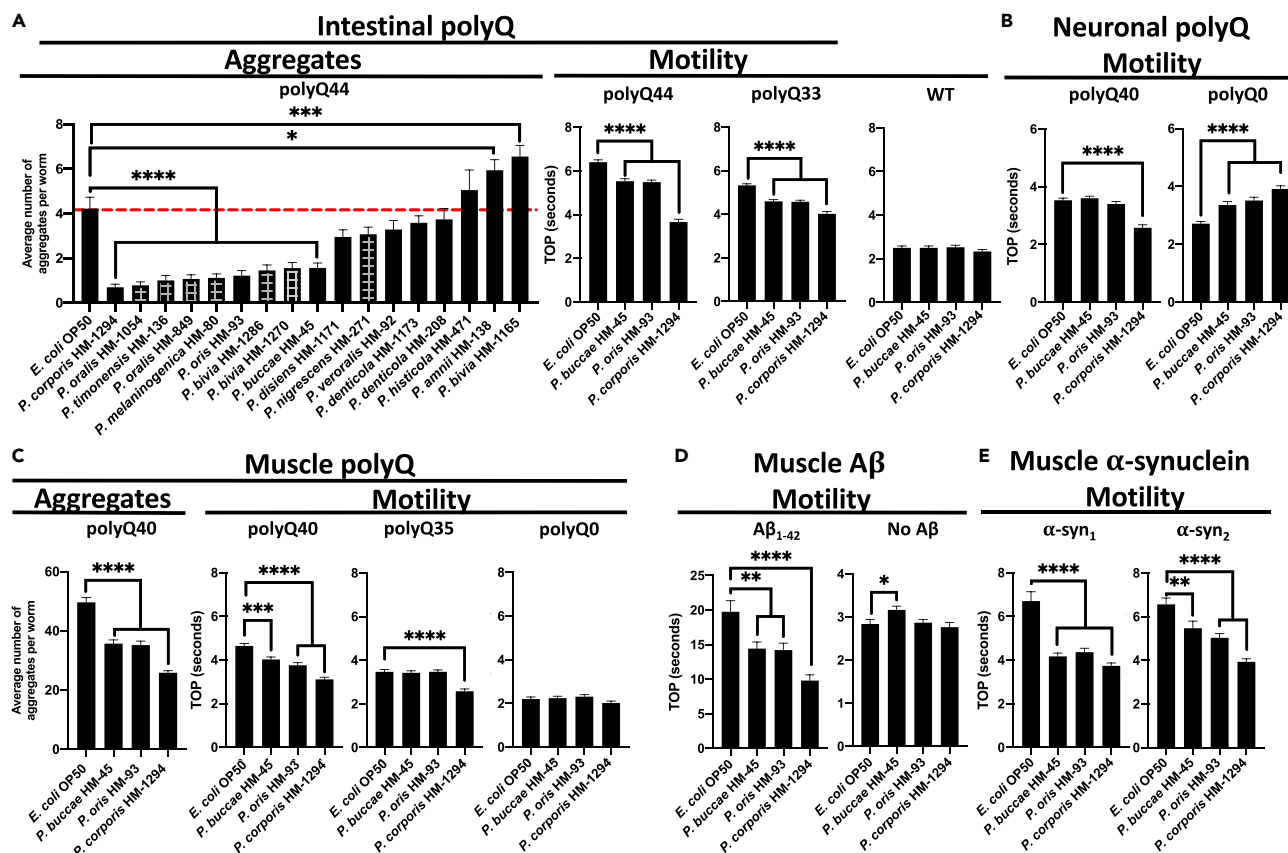


Figure 3. The effect of *Prevotella* spp. on proteins associated with neurodegenerative diseases

(A) The effect of *Prevotella* spp. on *C. elegans* intestinal polyQ aggregation (“Aggregates”) and the associated toxicity (“Motility”). Checkered bars represent bacteria-associated developmental delay. The three strongest suppressors of polyQ aggregation that did not affect development were tested using intestinal polyQ, (B) neuronal polyQ, (C) muscle polyQ, (D) muscle A β_{1-42} , and (E) muscle α -synuclein. Data are represented as the average number of aggregates or TOP (seconds) per worm obtained from at least two independent experiments for a total of 30–60 worms. Error bars represent standard error of the mean (SEM). Statistical significance was calculated using one-way ANOVA followed by multiple comparison Dunnett’s post-hoc test (* $p < 0.05$, ** $p < 0.01$, *** $p < 0.001$, **** $p < 0.0001$).

affect worm development, which is known to influence proteostasis.²⁸ We found that *Ralstonia* sp., *A. xylosoxidans*, *Pseudomonas* sp., and *Klebsiella pneumoniae* were the strongest inducers of polyQ aggregation (Figure 4A). As we have already demonstrated the proteotoxic potential of *P. aeruginosa* in our previous work,^{16,24} we focused on the three remaining species in follow-up experiments. To assess the proteotoxic effect of these bacteria, we employed the TOP assay to measure the motility of worms expressing aggregating polyQ44 and non-aggregating polyQ33. While we detected a significant enhancement in the motility defect in animals expressing polyQ44, no significant changes were observed in wild-type or animals expressing polyQ33 (Figure 4A). These results indicate that the impairment of motility induced by bacteria is contingent on polyQ aggregation rather than general bacterial pathogenicity. The aggregate-dependent motility defects were also observed in worms expressing neuronal and muscle-specific polyQ; however, the phenotype was less robust and we did detect some decrease in motility in control animals (Figures 4B and 4C). *A. xylosoxidans* also elevated muscle-specific polyQ aggregation (Figure 4C). To test the microbial influence on other disease-associated proteins, we employed worms expressing muscle-specific A β_{1-42} and α -synuclein. *A. xylosoxidans* induced proteotoxicity associated with both proteins (Figure 4D), and all three strains induced proteotoxicity associated with α -synuclein (Figure 4E). To determine whether the observed proteotoxicity is attributed to increased bacterial colonization, we quantified intestinal bacteria. Our results revealed that *K. pneumoniae*, *Ralstonia* sp., and *A. xylosoxidans* colonized less than *E. coli* OP50 (Figure S6), indicating that the proteotoxicity mediated by these strains is not explained by their colonization efficiencies. To delve deeper into the mechanism that underlies the bacterial proteotoxicity, we built upon our previous study that implicated secreted bacterial products in host proteotoxicity,²⁴ and exposed worms to spent culture supernatants from *K. pneumoniae* and *A. xylosoxidans*, two most robust inducers of polyQ aggregation. Our results revealed that supernatants from these bacteria significantly increased polyQ aggregation, whereas supernatants from *P. corporis* and *E. coli* OP50 had no effect (Figure S7). These results are intriguing as they suggest that the mechanism by which bacteria disrupt protein stability may involve secreted factors that can induce protein aggregation in proximal and distal tissues. Additionally, we

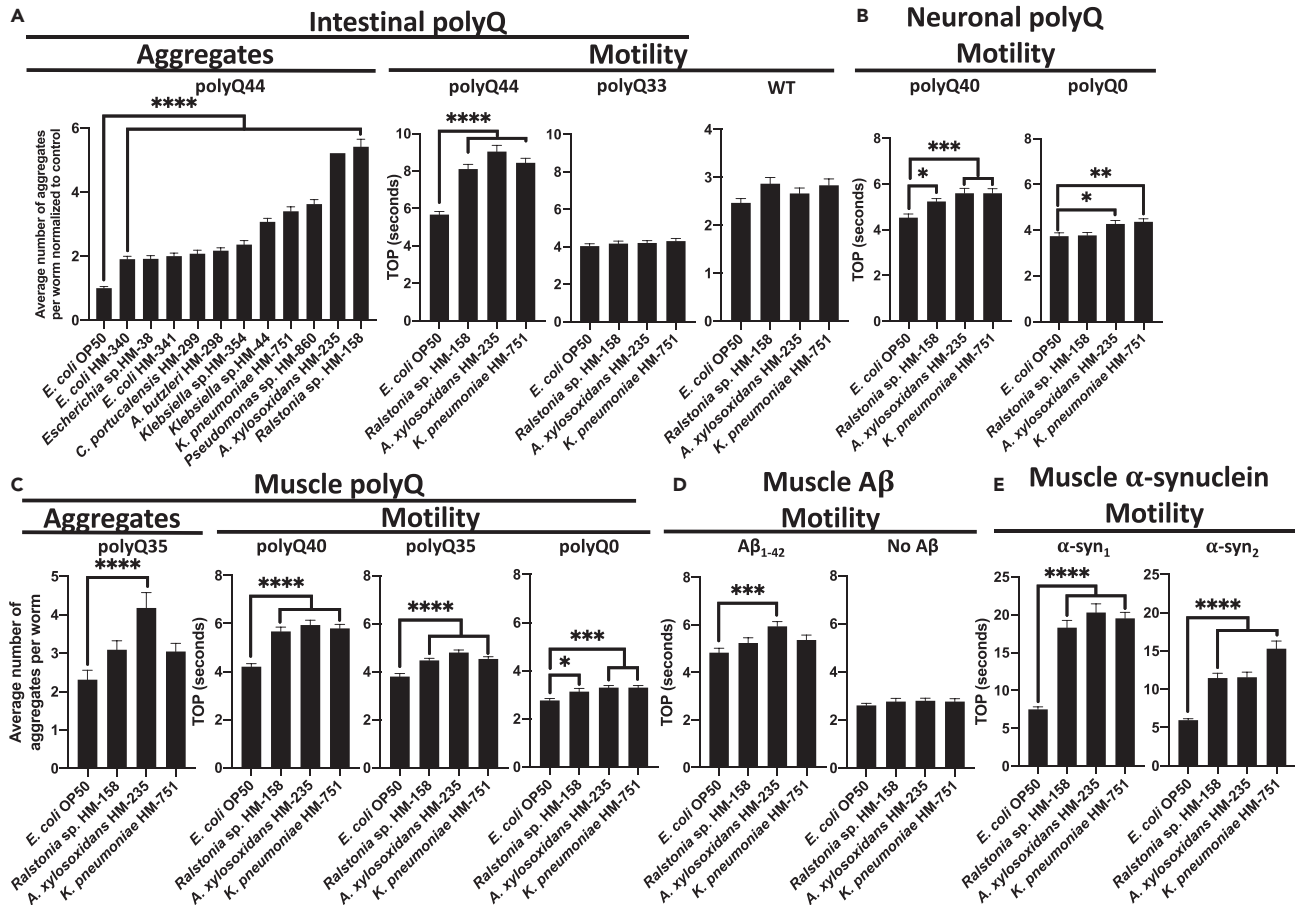


Figure 4. The effect of proteotoxic bacteria on proteins associated with neurodegenerative diseases

(A) The effect of gram-negative, aerobic bacteria on *C. elegans* intestinal polyQ aggregation (“Aggregates”) and the associated toxicity (“Motility”). Three robust enhancers of polyQ aggregation were tested using intestinal polyQ, (B) neuronal polyQ, (C) muscle polyQ, (D) muscle Aβ₁₋₄₂, and (E) muscle α-synuclein. Data are represented as the average number of aggregates or TOP (seconds) per worm obtained from at least two independent experiments for a total of 30–60 worms. Data in (A) (Aggregates) are normalized to worms fed the control *E. coli* OP50. Error bars represent SEM. Statistical significance was calculated using one-way ANOVA followed by multiple comparison Dunnett’s post-hoc test (**p* < 0.05, ***p* < 0.01, ****p* < 0.001, *****p* < 0.0001).

demonstrate that bacteria can enhance the proteotoxicity of diverse disease-associated proteins, supporting their role in the pathogenesis of neurodegenerative PCDs.

The human microbiota is composed of a diverse array of bacterial species that coexist and interact within a complex polymicrobial community. As such, we investigated the potential of a proteoprotective species to mitigate bacterial proteotoxicity by co-colonizing worms with *P. corporis* and either *K. pneumoniae* or *E. coli* OP50. Our findings revealed that *P. corporis* suppressed the polyQ aggregation associated with *K. pneumoniae* and *E. coli* OP50 (Figures 5A and 5B). We tested whether the same suppressive effect would result from co-colonizing worms with *K. pneumoniae* and *E. coli* OP50 and found that the resulting aggregation profile was an integrative reflection of the individual effects observed when each strain was introduced in isolation (Figure 5C). Collectively, these results indicate that, in addition to suppressing proteotoxicity from intrinsic factors like aging and host-encoded metastable proteins, *P. corporis* also suppresses host proteotoxicity mediated by extrinsic factors such as proteotoxic bacteria.

To investigate the mechanistic basis behind the ability of *P. corporis* to safeguard against host proteotoxicity, we explored its potential to activate the heat shock response (HSR), a critical and evolutionary conserved cellular defense mechanism that responds to protein misfolding and proteotoxic stress. Using *C. elegans* expressing a transcriptional fluorescent reporter, *hsp70p::GFP*, we monitored HSR activation in worms fed *P. corporis*. While control *E. coli* OP50 and proteotoxic *K. pneumoniae* did not elicit any detectable response, we found that *P. corporis* induced the reporter, indicating robust HSR activation (Figure 5D). This result highlights a potential mechanism by which bacteria can alleviate proteotoxicity in the host by activating protective stress responses. To our knowledge, this is the first documentation of bacterial induction of a protective HSR in the host, which opens new opportunities for bacteria-mediated therapeutic strategies against PCDs.

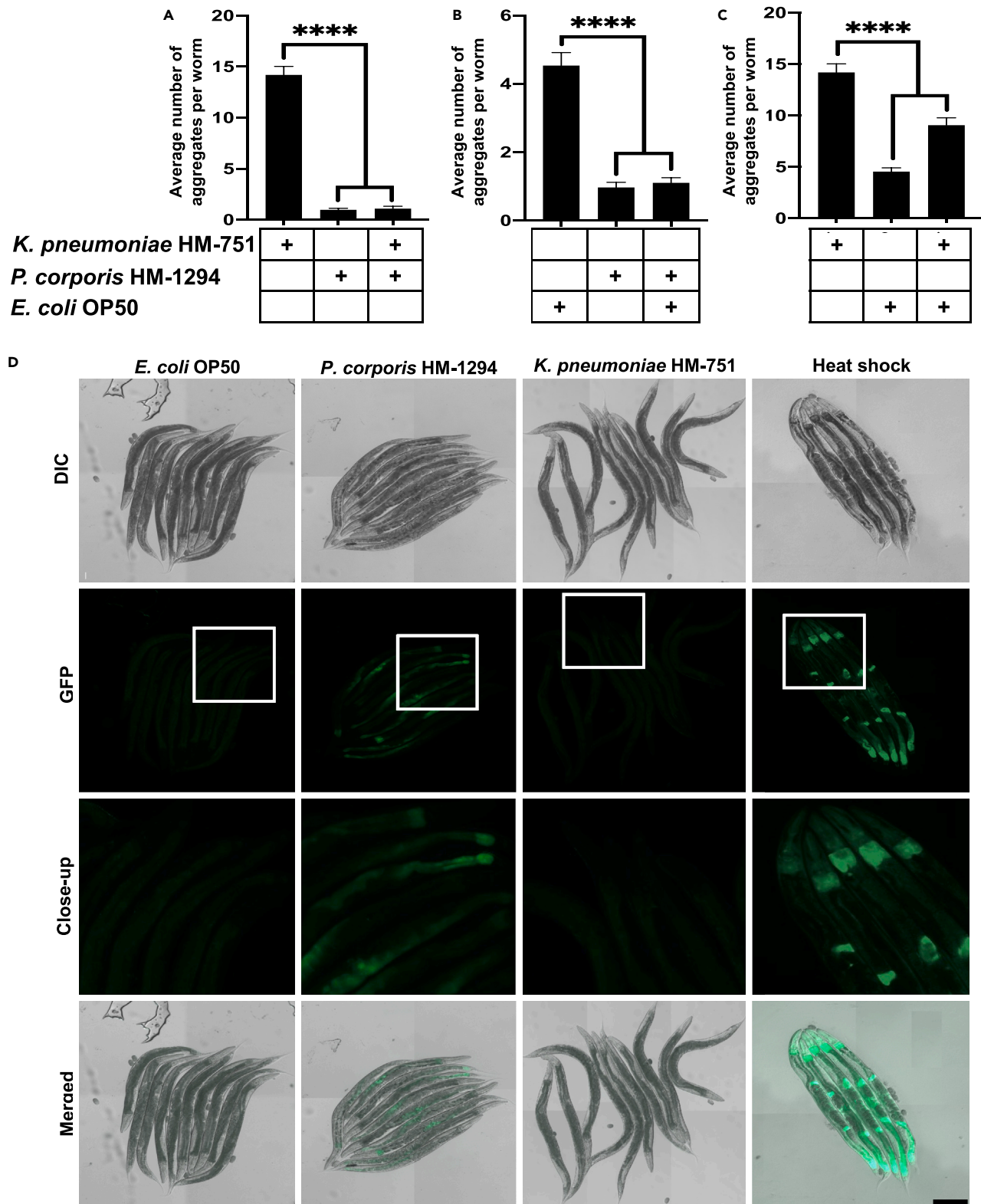


Figure 5. The effect of *P. corporis* on bacteria-induced polyQ aggregation and activation of the heat-shock response

(A–C) The effect of co-colonizing intestinal polyQ44 worms with (A) *K. pneumoniae* HM-751 and *P. corporis* HM-1294, (B) *E. coli* OP50 and *P. corporis* HM-1294, (C) *K. pneumoniae* HM-751 and *E. coli* OP50. Data are represented as the average number of aggregates per intestinal polyQ44 worm obtained from three

Figure 5. Continued

independent experiments for a total of 60 worms. Statistical significance was calculated using one-way analysis of variants (ANOVA) followed by multiple comparison Dunnett's post-hoc test (**** $p < 0.0001$).

(D) Nomarski and fluorescent (EGFP) images of transgenic worms expressing transcriptional fusion reporter *hsp70p::GFP*, fed *E. coli* OP50, *P. corporis* HM-1294, *K. pneumoniae* HM-751, and as a positive control, heat-shocked worms fed *E. coli* OP50. Scale bar is 200 μm .

DISCUSSION

In the present study, we screened a comprehensive collection of 229 unique bacterial isolates from the Human Microbiome Project for their ability to affect host proteostasis from within the intestinal milieu. Our follow-up experiments on the most robust beneficial and detrimental bacteria confirmed their influence on proteostasis across host tissues, affecting the stability of proteins associated with Alzheimer's, Parkinson's, and Huntington's diseases. The phylogenetic analysis revealed clustering of select proteotoxic and proteoprotective bacteria, indicating that genetically related bacteria affect host proteostasis in a similar manner, but with a different magnitude (Figure S8). To our knowledge, this is the first comprehensive characterization of bacteria from human microbiomes on host proteostasis. Surprisingly, our data suggest that bacteria do not selectively target any specific host proteins associated with PCDs, but rather affect proteostasis in general, leading to the aggregation and proteotoxicity of any destabilized proteins present within the proteome, such as exogenous polyQ, $A\beta_{1-42}$, and α -synuclein, tested in our experiments. While this is a generalized mechanism, there could be microbes that exclusively affect a specific disease.

Numerous studies that employed genomic analyses of microbial compositions in affected patients revealed a connection between comparable gut dysbioses and diverse neurodegenerative PCDs.⁶ These correlational studies from human subjects support our conclusion that bacteria impact host protein stability by modulating host proteostasis. This mechanism is likely mediated by the interplay between host proteostasis and immune responses to bacteria.^{29,30}

Many of the studies aiming to identify neurodegenerative PCD etiology or treat the disease have concentrated on host-targeted therapeutics, primarily focused on targeting the aggregating proteins or the affected cell types. However, this approach has not been successful in pre-clinical or clinical trials.^{31,32} Perhaps the focal point of the host-targeted approach occurs too late in the aggregation cascade given that the changes in the gut microbiota can happen prior to any clinical manifestation.^{33,34} Indeed, individuals with neurodegenerative PCDs have insufficient proteostatic capacity.³⁵ While some studies have attempted to treat neurodegenerative PCDs by enhancing components of the host proteostasis network, these have not been successful.³¹ In support of our results indicating that bacteria affect host proteostasis, a shift toward microbial-centered therapeutic approaches has shown more promise in lessening disease symptoms. For example, eradication of *Helicobacter pylori* in AD patients was associated with improved disease presentation in a clinical trial and a population-based study.^{36,37} Interestingly, the beneficial effect of antibiotics on the progression of PCDs, when administered post-onset, is absent when antibiotics were used prior to disease onset; notably, general antibiotic use has been associated with increased risk for PCDs as well as gut dysbiosis.^{38–40} While *H. pylori* is a good clinical example of microbial contribution to neurodegenerative diseases, we did not expect to detect proteotoxicity associated with this bacterium in our *C. elegans* model due to a limitation of our approach that includes transferring and incubating bacteria at sub-optimal temperature—a factor that facilitates *H. pylori* virulence.⁴¹ Additional reports suggest that *H. pylori* can indirectly affect the composition of the human gut microbiota.⁴² Microbe-targeted therapeutic approaches hold promise and are further bolstered by a recent study that demonstrated that gut microbiota and serum derived from AD patients accelerate disease symptoms and affect neurogenesis in healthy rats and tissue culture, respectively.⁴³

In our screen (Figure 2), *Prevotella* stood out as the only genus devoid of any species that exhibit proteotoxicity toward the host. Furthermore, our findings indicate that *Prevotella* spp. have a broad and suppressive effect on host protein aggregation, regardless of the specific disease-associated protein (Figure 3). Sequencing data suggest that a low abundance of *Prevotella* in the guts of patients with PCDs enhances disease pathogenesis.^{7–14} However, despite the fact that the *Prevotella* genus contains over 50 species, many studies report their results at the genus level.⁴⁴ Our data indicate that various *Prevotella* species exhibit a differential effect on host proteostasis (Figure 3A). Such various effects of individual species could be explained by large variability in their genomes.⁴⁴ The species, *P. intermedia*, *P. nigrescense*, and *P. melanigencia* have been consistently associated with infection,^{45–47} inflammation,^{48–51} and have also been linked to AD and associated mortality.⁵² Conversely, it has been shown that *P. buccae* and *P. corporis*, two strains of *Prevotella* that exhibited strong suppression of protein aggregation and the associated toxicity in the present study, were found not to induce inflammation.⁵³ Instead, *P. buccae* and *P. corporis* were shown to induce the expression of mucin-associated membrane proteins MUC3 and MUC4.⁵³ Interestingly, induction of MUC3 expression by a probiotic cocktail prevented adherence of enteropathogenic *E. coli*.⁵⁴ MUC4 has been shown to be essential for maintaining mucus barrier function and intestinal homeostasis in mice, as its absence resulted in severe large intestinal bleeding and significant down-regulation of antimicrobial peptides.⁵⁵ Though preliminary, the evidence suggesting the protective role of *Prevotella* in maintaining intestinal integrity is interesting, as intestinal integrity is often compromised in people with neurodegenerative PCDs.⁵⁶ Damage to the intestinal epithelium can lead to translocation of bacteria and bacterial products, resulting in systemic inflammation and the breakdown of the blood-brain barrier, contributing to a variety of diseases, including PCDs.^{57,58} The translocation of bacterial products becomes even more relevant given our results showing the proteotoxic effect of secreted bacterial factors (Figure S7). The contrasting associations of different *Prevotella* species in host health and disease highlight the importance of studying bacteria at the species level, as demonstrated in the present study, to unravel the precise roles of bacteria in disease pathogenesis. The *Bacillus* genus is another example that supports the need for species-level studies, as this genus encompasses diverse species that exhibit opposing effects on the host; *Bacillus anthracis* is a controlled bioweapon,⁵⁹ whereas

Bacillus subtilis is a probiotic that has been shown to play a protective role against the aggregation of α -synuclein in *C. elegans*, partly through its metabolites.⁶⁰

The physiological relevance of our findings is supported by studies that focus on pathogenic bacteria and subsequently establish a connection with PCDs. For example, the robust induction of proteotoxicity by *K. pneumoniae* in *C. elegans* models expressing different aggregation-prone proteins (Figure 4) is in agreement with a previous study that identified an overabundance of *K. pneumoniae* in the gut microbiota of individuals with AD.⁶¹ Furthermore, a positive correlation has been demonstrated between the presence of *K. pneumoniae* in the gut and elevated levels of the AD-associated biomarker, C-reactive protein, in blood samples of AD patients.⁶² Another study found an elevated abundance of *Ralstonia* in mucosal samples from individuals with PD,⁶³ which is another bacterium that was robustly proteotoxic to our *C. elegans* models (Figure 4). Interestingly, this bacterium was also found to be more prevalent in individuals with autism,⁶⁴ which is another disease that has been associated with the presence of misfolded proteins.^{65–68} Autism has also been associated with both *Achromobacter* and *Pseudomonas* genera.^{69,70} Both *Achromobacter* and *Pseudomonas* are linked to cystic fibrosis (CF), which is another PCD that does not feature neurodegeneration;^{71,72} *Achromobacter* was reported to exacerbate the disease,⁷³ and *P. aeruginosa* is a predominant pathogenic species that colonizes the lungs of CF patients.⁷⁴ *A. xylosoxidans* induced proteotoxicity in all our disease models (Figure 4), and *Pseudomonas* notably increased polyQ aggregation (Figure 4A, "Aggregates"). Furthermore, we previously demonstrated that *P. aeruginosa* exerts robust proteotoxic effects on *C. elegans*.^{16,24} The presence of *Pseudomonas*, in conjunction with another bacterial genus, was successfully used to differentiate individuals with AD from control subjects.⁷⁵ Collectively, the aforementioned studies are in agreement with our results and further support the wide-ranging impact of bacteria on protein-folding diseases. It is remarkable that the abovementioned bacteria induce proteotoxicity consistently across our *C. elegans* models expressing distinct disease proteins. The convergence of our results with existing literature linking these bacteria to PCDs strongly reinforces the notion that bacteria affect the host proteostasis network, broadly affecting protein stability and, consequently, disease pathogenesis.

While our results support a wider-reaching impact of bacteria on the stability of host proteins, it is worth noting that bacteria can selectively target components of the host proteostasis network. This notion is supported by our data showing that *P. corporis* acts as a potent protector against host proteotoxicity (Figures 3, 5A, 5B, S4, and S5) and an activator of the HSR (Figure 5D). Reports demonstrating that activation of the HSR leads to a reduction of protein aggregation support our findings,⁷⁶ suggesting that activation of the HSR is a mechanism through which *P. corporis* confers proteoprotection to the host. Another example of bacterial influence on host proteostasis is illustrated by *P. aeruginosa*, which produces toxins that target the mitochondrial unfolded protein response (UPR^{MT}),⁷⁷ a transcriptional pathway that ensures proper protein folding and clearance.⁷⁸ As such, when the UPR^{MT} is overwhelmed or disrupted, proteotoxicity can occur, leading to accelerated protein aggregation.⁷⁹ Our previous work demonstrated that *P. aeruginosa* and *E. coli* can also disrupt host proteostasis through the production of bacteria-derived protein aggregates.^{16,24} Additionally, *P. aeruginosa* FapC amyloids were shown to cross-seed with A β _{1–42}.⁸⁰ Interestingly, the *fap* operon is also present in the genomes of Burkholderiales, which include *Ralstonia* and *Achromobacter*.^{81,82} The *E. coli* amyloid, curli, enhanced the aggregation of α -synuclein *in vivo*.⁸³ *K. pneumoniae* is also capable of producing amyloids,⁸⁴ and was proteotoxic to all *C. elegans* lines (Figure 4). The underlying mechanisms of the bacteria-induced proteotoxicity remain elusive; however, it is likely that metastable proteins of bacterial origin sequester host chaperones. Such sequestration would diminish the capacity of the proteostasis network to buffer the folding of endogenous proteins. A similar mechanism is supported by the organismal ability to buffer protein polymorphisms present within the host proteome, which is hindered by the introduction of misfolded proteins.⁸⁵

Another way bacteria can cause proteotoxicity in their host is through inflammation, which initiates a cascade where disrupted proteostasis amplifies inflammation and perpetuates a continuous cycle.³⁰ Bacteria have the capacity to stimulate the generation and release of reactive oxygen and nitrogen species, which trigger inflammation and have the potential to disrupt host proteostasis.³⁰ Moreover, the endotoxin hypothesis of neurodegeneration postulates that endotoxin from the gut can breach the blood-brain barrier and trigger neuroinflammation and neurodegeneration.^{86,87} This process is thought to be initiated by bacterial dysbiosis, leading to an increase in gram-negative bacterial species that contribute to systemic inflammation.

Maintaining a balanced microbiome is critical for human health and longevity. However, the microbial equilibrium can be disrupted by many factors, including the overgrowth of pathogenic bacteria and antimicrobial use, leading to a state of gut dysbiosis. Notably, *Prevotella* spp., which we demonstrated to have a proteoprotective effect (Figure 3), can be depleted by antimicrobial use.³⁰ Conversely, the proteotoxic bacteria identified in our study, *A. xylosoxidans*, *K. pneumoniae*, and *Ralstonia* sp. (Figure 4), are resistant to many antibiotics.^{82,88–91} This raises a new concern in the current era of increasing antimicrobial resistance, as poor antimicrobial stewardship might enrich not only for multidrug-resistant bacteria, but also for multidrug-resistant bacteria that are proteotoxic and pose potential risk factors for neurodegenerative disease. The implications of antibiotic-induced gut dysbiosis on PCD pathogenesis become particularly intriguing when corroborated with our data showing that *P. corporis* completely inhibited the proteotoxicity of *K. pneumoniae* (Figure 5A). However, *P. corporis* alone also protected the host against proteotoxicity (Figure 3), suggesting that beneficial bacteria may serve an additional role by counteracting the detrimental effects on host proteins induced by other bacterial species. While our data indicate the protection is likely due to *P. corporis* enhancing the host's capacity to effectively manage bacteria-induced proteotoxicity through activation of the HSR (Figure 5D), it is possible that the presence of *P. corporis* also directly hinders the detrimental potential of proteotoxic bacteria. Ongoing research is aimed at elucidating the precise signals and mechanisms by which *P. corporis* exerts its protective effects.

The clinical relevance of our findings, which suggest a protective role of *P. corporis* against protein misfolding and aggregation by suppressing bacteria-induced proteotoxicity and activation of the host HSR (Figure 5D), is bolstered by previous literature that links decreased *Prevotella* abundance with exacerbated PCD.^{7–14} This is further supported by studies that implicate the HSR as a promising therapeutic target

for neurodegenerative disease. For example, several studies observed a reduction in AD risk with moderate to frequent sauna bathing, suggesting that intermittent, temperature-induced activation of the HSR protects against proteotoxicity,^{92,93} a mechanism that has been demonstrated in *C. elegans*.⁹⁴ Intranasal administration of human chaperone HSP70 improved AD-like symptoms in two mouse models of AD.⁹⁵ Treatment of ALS mice with arimoclomol, a drug that increases the levels of HSP70 by interacting with the HSR transcription factor, heat shock factor-1 (HSF-1),⁹⁶ delayed disease progression.⁹⁷ Additionally, a study demonstrated that the cytoprotective effect of the FDA-approved ALS drug, riluzole, is dependent on its ability to increase cytosolic HSF-1.⁹⁸ Collectively, the abovementioned research implicating activation of the HSR as an intervention strategy for neurodegenerative diseases reinforces the clinical importance of our findings linking the ability of *P. corporis* to suppress proteotoxicity and activate the HSR in its host. To our knowledge, this is the first-ever report of bacteria inducing a protective stress response in the host. Such a finding bolsters the feasibility of a microbial management strategy to treat neurodegenerative disease.

A comprehensive understanding of individual bacterial residents of the human microbiota in the pathogenesis of neurodegenerative PCDs is crucial in developing effective interventions. Our study challenges the traditional approach of solely focusing on host-targeted therapeutics for neurodegenerative PCDs. Instead, modulating the gut microbiota may offer an effective strategy for preventing and managing these devastating diseases. Gut-targeted interventions will likely have to be implemented early in the disease or even prior to its onset. While our results indicate that bacteria generally affect host proteostasis, ultimately influencing the stability of host proteins, further studies are needed to decipher the role of proteoprotective and proteotoxic species in humans and devise approaches to control their levels.

Limitations of the study

Our study has several limitations that need to be acknowledged. First, using *C. elegans* as a model organism may not fully recapitulate the complexity of human neurodegenerative diseases. A major limitation of our study is the temperature at which nematodes are cultured. While worms grow at the optimal temperatures of 15°C–25°C, bacteria that colonize the human gut are exposed to human body temperature. As such, it is possible that specific factors, either beneficial or detrimental, are not synthesized by bacteria at temperatures lower than 37°C. Our single bacterial strain approach also has limitations in that it does not capture the complexity of the microbial interactions within the human gut microbiota. Furthermore, our study addresses the short-term effect of bacterial colonization, but the long-term effects will have to be explored using other models with longer lifespans. Despite these limitations, our approach and model are best suited to our specific research objectives, and the results are supported by correlational studies observed in patients with neurodegenerative diseases.

RESOURCE AVAILABILITY

Lead contact

Additional information and request for resources should be directed to and will be fulfilled by lead contact, Daniel M. Czyż (dczyz@ufl.edu).

Materials availability

This study did not generate new unique reagents.

Data and code availability

- All data reported in this paper will be shared by the lead author upon request.
- This paper does not report original code.
- Any additional information required to reanalyze the data reported in the paper is available from the [lead contact](#) upon request.

ACKNOWLEDGMENTS

We thank Dr. Richard Morimoto and Sue Fox for providing *C. elegans* polyQ strains (Northwestern University), and Dr. Janine Kirstein (Leibniz Institute on Aging – Fritz Lipmann Institute) for providing the *C. elegans* Aβ₁₋₄₂ strain and the "No Aβ" control. All other *C. elegans* strains were provided by the Caenorhabditis Genetics Center, which is funded by the NIH Office of Research Infrastructure Programs (P40 OD010440). Human bacterial isolates (listed in [Table S1](#)) were obtained through BEI Resources, NIAID, and NIH as part of the Human Microbiome Project. We thank Dr. Mark Gorelik for training RB and for assistance with computational analysis. We would like to thank the funders who have supported our work on the bacterial contribution to protein conformational diseases, namely the National Institute on Aging (R03AG070580), the Infectious Diseases Society of America – Microbial Pathogenesis in Alzheimer's Disease, the Glenn Foundation for Medical Research, and AFAR Grant for Junior Faculty. Furthermore, we acknowledge and thank the Department of Microbiology and Cell Science for start-up funding. The graphical abstract and [Figure 1](#) were created using [BioRender.com](#).

AUTHOR CONTRIBUTIONS

Conceptualization: D.M.C.; methodology: A.C.W. and D.M.C.; software: R.B. and M.J.B.; validation: A.C.W., R.B., Y.M.A., and A.S.B.; formal analysis: A.C.W. and D.M.C.; investigation: D.M.C., A.C.W., R.B., Y.M.A., and A.S.B.; resources: D.M.C.; writing – original draft: A.C.W. and D.M.C.; writing – reviewing & editing: A.C.W. and D.M.C.; visualization: A.C.W., R.B., and M.J.B.; supervision: D.M.C. and A.C.W.; project administration: D.M.C.; funding acquisition: D.M.C.

DECLARATION OF INTERESTS

The authors declare no competing interest.

STAR★METHODS

Detailed methods are provided in the online version of this paper and include the following:

- KEY RESOURCES TABLE
- EXPERIMENTAL MODEL AND STUDY PARTICIPANT DETAILS
 - *C. elegans* maintenance
- METHOD DETAILS
 - Bacterial culture conditions
 - Aggregate quantification
 - Motility assays
 - Feeding worms PFA-killed bacteria
 - Pharyngeal pumping
 - Exposing worms to bacterial supernatants
 - Co-colonization assays
 - Quantification of intestinal bacteria
 - Live imaging
 - Gel electrophoresis and western blotting
 - Heatmap generation
 - Phylogenetic tree generation
- QUANTIFICATION AND STATISTICAL ANALYSIS

SUPPLEMENTAL INFORMATION

Supplemental information can be found online at <https://doi.org/10.1016/j.isci.2024.110828>.

Received: October 24, 2023

Revised: April 5, 2024

Accepted: August 23, 2024

Published: August 27, 2024

REFERENCES

1. Soto, C. (2003). Unfolding the role of protein misfolding in neurodegenerative diseases. *Nat. Rev. Neurosci.* 4, 49–60. <https://doi.org/10.1038/nm1007>.
2. Alzheimers Dement (2022). Alzheimer's disease facts and figures. *J. Alzheimers Assoc.* 18, 700–789. <https://doi.org/10.1002/alz.12638>.
3. Oliphant, K., and Allen-Vercoe, E. (2019). Macronutrient metabolism by the human gut microbiome: major fermentation by-products and their impact on host health. *Microbiome* 7, 91. <https://doi.org/10.1186/s40168-019-0704-8>.
4. Clarke, G., Stilling, R.M., Kennedy, P.J., Stanton, C., Cryan, J.F., and Dinan, T.G. (2014). Minireview: Gut Microbiota: The Neglected Endocrine Organ. *Mol. Endocrinol.* 28, 1221–1238. <https://doi.org/10.1210/me.2014-1108>.
5. Intili, G., Paladino, L., Rappa, F., Alberti, G., Plicato, A., Calabrò, F., Fucarino, A., Cappello, F., Bucchieri, F., Tomasello, G., et al. (2023). From Dysbiosis to Neurodegenerative Diseases through Different Communication Pathways: An Overview. *Biology* 12, 195. <https://doi.org/10.3390/biology12020195>.
6. Fang, P., Kazmi, S.A., Jameson, K.G., and Hsiao, E.Y. (2020). The Microbiome as a Modifier of Neurodegenerative Disease Risk. *Cell Host Microbe* 28, 201–222. <https://doi.org/10.1016/j.chom.2020.06.008>.
7. Jin, M., Li, J., Liu, F., Lyu, N., Wang, K., Wang, L., Liang, S., Tao, H., Zhu, B., and Alkasis, R. (2019). Analysis of the Gut Microflora in Patients With Parkinson's Disease. *Front. Neurosci.* 13, 1184.
8. Scheperjans, F., Aho, V., Pereira, P.A.B., Koskinen, K., Paulin, L., Pekkonen, E., Haapaniemi, E., Kaakkola, S., Eerola-Rautio, J., Pohja, M., et al. (2015). Gut microbiota are related to Parkinson's disease and clinical phenotype. *Mov. Disord.* 30, 350–358. <https://doi.org/10.1002/mds.26069>.
9. Hertzberg, V.S., Singh, H., Fournier, C.N., Moustafa, A., Polak, M., Kuelbs, C.A., Torralba, M.G., Tansey, M.G., Nelson, K.E., and Glass, J.D. (2022). Gut microbiome differences between amyotrophic lateral sclerosis patients and spouse controls. *Amyotroph. Lateral Scler. Front. Degener.* 23, 91–99. <https://doi.org/10.1080/21678421.2021.1904994>.
10. Vidal-Martinez, G., Chin, B., Camarillo, C., Herrera, G.V., Yang, B., Sarosiek, I., and Perez, R.G. (2020). A Pilot Microbiota Study in Parkinson's Disease Patients versus Control Subjects, and Effects of FTY720 and FTY720-Mitoxoy Therapies in Parkinsonian and Multiple System Atrophy Mouse Models. *J. Park. Dis.* 10, 185–192. <https://doi.org/10.3233/JPD-191693>.
11. Unger, M.M., Spiegel, J., Dillmann, K.-U., Grundmann, D., Philippeit, H., Bürmann, J., Faßbender, K., Schwierz, A., and Schäfer, K.-H. (2016). Short chain fatty acids and gut microbiota differ between patients with Parkinson's disease and age-matched controls. *Parkinsonism Relat. Disord.* 32, 66–72. <https://doi.org/10.1016/j.parkrel.2016.08.019>.
12. Li, F., Wang, P., Chen, Z., Sui, X., Xie, X., and Zhang, J. (2019). Alteration of the fecal microbiota in North-Eastern Han Chinese population with sporadic Parkinson's disease. *Neurosci. Lett.* 707, 134297. <https://doi.org/10.1016/j.neulet.2019.134297>.
13. Bedarf, J.R., Hildebrand, F., Coelho, L.P., Sunagawa, S., Bahram, M., Goeser, F., Bork, P., and Wüllner, U. (2017). Functional implications of microbial and viral gut metagenome changes in early stage L-DOPA-naïve Parkinson's disease patients. *Genome Med.* 9, 39. <https://doi.org/10.1186/s13073-017-0428-y>.
14. Aho, V.T.E., Pereira, P.A.B., Voutilainen, S., Paulin, L., Pekkonen, E., Auvinen, P., and Scheperjans, F. (2019). Gut microbiota in Parkinson's disease: Temporal stability and relations to disease progression. *EBioMedicine* 44, 691–707. <https://doi.org/10.1016/j.ebiom.2019.05.064>.
15. Wallen, Z.D., Demirkan, A., Twa, G., Cohen, G., Dean, M.N., Standaert, D.G., Sampson, T.R., and Payami, H. (2022). Metagenomics of Parkinson's disease implicates the gut microbiome in multiple disease mechanisms. *Nat. Commun.* 13, 6958. <https://doi.org/10.1038/s41467-022-34667-x>.
16. Walker, A.C., Bhargava, R., Vaziriyani-Sani, A.S., Pourciau, C., Donahue, E.T., Dove, A.S., Gebhardt, M.J., Ellward, G.L., Romeo, T., and Czyż, D.M. (2021). Colonization of the *Caenorhabditis elegans* gut with human enteric bacterial pathogens leads to proteostasis disruption that is rescued by butyrate. *PLoS Pathog.* 17, e1009510. <https://doi.org/10.1371/journal.ppat.1009510>.
17. Walker, A.C., Bhargava, R., Brust, A.S., Owji, A.A., and Czyż, D.M. (2022). Time-off-pick Assay to Measure *Caenorhabditis elegans* Motility. *Bio. Protoc.* 12, e4436. <https://doi.org/10.21769/BioProtoc.4436>.
18. Steinkraus, K.A., Smith, E.D., Davis, C., Carr, D., Pendergrass, W.R., Sutphin, G.L., Kennedy, B.K., and Kaerberlein, M. (2008). Dietary restriction suppresses proteotoxicity and enhances longevity by an hsf-1-dependent mechanism in *Caenorhabditis elegans*. *Aging Cell* 7, 394–404. <https://doi.org/10.1111/j.1474-9726.2008.00385.x>.

19. Bodhicharla, R., Nagarajan, A., Winter, J., Adenle, A., Nazir, A., Brady, D., Vere, K., Richens, J., O'Shea, P., Bell, D.R., and de Pomerai, D. (2012). Effects of α -Synuclein Overexpression in Transgenic *Caenorhabditis elegans* Strains. *CNS Neurol. Disord.: Drug Targets* 11, 965–975. <https://doi.org/10.2174/1871527311211080005>.
20. van Ham, T.J., Thijssen, K.L., Breitling, R., Hofstra, R.M.W., Plasterk, R.H.A., and Nollen, E.A.A. (2008). *C. elegans* Model Identifies Genetic Modifiers of α -Synuclein Inclusion Formation During Aging. *PLoS Genet.* 4, e1000027. <https://doi.org/10.1371/journal.pgen.1000027>.
21. Gallrein, C., Iburg, M., Michelberger, T., Koçak, A., Puchkov, D., Liu, F., Ayala Mariscal, S.M., Nayak, T., Kaminski Schierle, G.S., and Kirstein, J. (2021). Novel amyloid-beta pathology *C. elegans* model reveals distinct neurons as seeds of pathogenicity. *Prog. Neurobiol.* 198, 101907. <https://doi.org/10.1016/j.pneurobio.2020.101907>.
22. Morley, J.F., Brignull, H.R., Weyers, J.J., and Morimoto, R.I. (2002). The threshold for polyglutamine-expansion protein aggregation and cellular toxicity is dynamic and influenced by aging in *Caenorhabditis elegans*. *Proc. Natl. Acad. Sci. USA* 99, 10417–10422. <https://doi.org/10.1073/pnas.152161099>.
23. Taylor, R.C., and Dillin, A. (2011). Aging as an event of proteostasis collapse. *Cold Spring Harb. Perspect. Biol.* 3, a004440. <https://doi.org/10.1101/cshperspect.a004440>.
24. Walker, A.C., Bhargava, R., Dove, A.S., Brust, A.S., Owji, A.A., and Czyz, D.M. (2022). Bacteria-Derived Protein Aggregates Contribute to the Disruption of Host Proteostasis. *Int. J. Mol. Sci.* 23, 4807. <https://doi.org/10.3390/ijms23094807>.
25. Ben-Zvi, A., Miller, E.A., and Morimoto, R.I. (2009). Collapse of proteostasis represents an early molecular event in *Caenorhabditis elegans* aging. *Proc. Natl. Acad. Sci. USA* 106, 14914–14919. <https://doi.org/10.1073/pnas.0902882106>.
26. Macleod, A.R., Waterston, R.H., Fishpool, R.M., and Brenner, S. (1977). Identification of the structural gene for a myosin heavy-chain in *Caenorhabditis elegans*. *J. Mol. Biol.* 114, 133–140. [https://doi.org/10.1016/0022-2836\(77\)90287-X](https://doi.org/10.1016/0022-2836(77)90287-X).
27. Clark, S.G., Shurland, D.-L., Meyerowitz, E.M., Bargmann, C.I., and van der Bliek, A.M. (1997). A dynamin GTPase mutation causes a rapid and reversible temperature-inducible locomotion defect in *C. elegans*. *Proc. Natl. Acad. Sci. USA* 94, 10438–10443.
28. Labbadia, J., and Morimoto, R.I. (2014). Proteostasis and longevity: when does aging really begin? *FI000Prime Rep.* 6, 7. <https://doi.org/10.12703/P6-7>.
29. Tansey, M.G., Wallings, R.L., Houser, M.C., Herrick, M.K., Keating, C.E., and Joers, V. (2022). Inflammation and immune dysfunction in Parkinson disease. *Nat. Rev. Immunol.* 22, 657–673. <https://doi.org/10.1038/s41577-022-00684-6>.
30. Walker, A., and Czyz, D.M. (2023). Oh my gut! Is the microbial origin of neurodegenerative diseases real? *Infect. Immun.* 91, e0043722. <https://doi.org/10.1128/iai.00437-22>.
31. Sweeney, P., Park, H., Baumann, M., Dunlop, J., Frydman, J., Kopito, R., McCampbell, A., Leblanc, G., Venkateswaran, A., Nurmi, A., and Hodgson, R. (2017). Protein misfolding in neurodegenerative diseases: implications and strategies. *Transl. Neurodegener.* 6, 6. <https://doi.org/10.1186/s40035-017-0077-5>.
32. Mullane, K., and Williams, M. (2019). Preclinical Models of Alzheimer's Disease: Relevance and Translational Validity. *Curr. Protoc. Pharmacol.* 84, e57. <https://doi.org/10.1002/cpph.57>.
33. Savica, R., Carlin, J.M., Grossardt, B.R., Bower, J.H., Ahlsgog, J.E., Maraganore, D.M., Bharucha, A.E., and Rocca, W.A. (2009). Medical records documentation of constipation preceding Parkinson disease. *Neurology* 73, 1752–1758. <https://doi.org/10.1212/WNL.0b013e3181c34af5>.
34. Ferreira, A.L., Choi, J., Ryou, J., Newcomer, E.P., Thompson, R., Bollinger, R.M., Hall-Moore, C., Ndao, I.M., Sax, L., Benzinger, T.L.S., et al. (2023). Gut microbiome composition may be an indicator of preclinical Alzheimer's disease. *Sci. Transl. Med.* 15, eabo2984. <https://doi.org/10.1126/scitranslmed.abo2984>.
35. Tseng, C.-S., Chao, Y.-W., Liu, Y.-H., Huang, Y.-S., and Chao, H.-W. (2023). Dysregulated proteostasis network in neuronal diseases. *Front. Cell Dev. Biol.* 11, 1075215. <https://doi.org/10.3389/fcell.2023.1075215>.
36. Chang, Y.-P., Chiu, G.-F., Kuo, F.-C., Lai, C.-L., Yang, Y.-H., Hu, H.-M., Chang, P.-Y., Chen, C.-Y., Wu, D.-C., and Yu, F.-J. (2013). Eradication of *Helicobacter pylori* Is Associated with the Progression of Dementia: A Population-Based Study. *Gastroenterol. Res. Pract.* 2013, e175729. <https://doi.org/10.1155/2013/175729>.
37. Kountouras, J., Boziki, M., Gavalas, E., Zavos, C., Grigoriadis, N., Deretzi, G., Tzilves, D., Katsinelos, P., Tsolaki, M., Chatzopoulos, D., and Venizelos, I. (2009). Eradication of *Helicobacter pylori* may be beneficial in the management of Alzheimer's disease. *J. Neurol.* 256, 758–767. <https://doi.org/10.1007/s00415-009-5011-z>.
38. Elvers, K.T., Wilson, V.J., Hammond, A., Duncan, L., Huntley, A.L., Hay, A.D., and van der Werf, E.T. (2020). Antibiotic-induced changes in the human gut microbiota for the most commonly prescribed antibiotics in primary care in the UK: a systematic review. *BMJ Open* 10, e035677. <https://doi.org/10.1136/bmjopen-2019-035677>.
39. Sun, J., Zhan, Y., Mariosa, D., Larsson, H., Almqvist, C., Ingre, C., Zagai, U., Pawitan, Y., and Fang, F. (2019). Antibiotics use and risk of amyotrophic lateral sclerosis in Sweden. *Eur. J. Neurol.* 26, 1355–1361. <https://doi.org/10.1111/ene.13986>.
40. Mertsalmi, T.H., Pekkonen, E., and Scheperjans, F. (2020). Antibiotic exposure and risk of Parkinson's disease in Finland: A nationwide case-control study. *Mov. Disord.* 35, 431–442. <https://doi.org/10.1002/mds.27924>.
41. Goodwin, C.S., and Armstrong, J.A. (1990). Microbiological aspects of *Helicobacter pylori* (Campylobacter pylori). *Eur. J. Clin. Microbiol. Infect. Dis.* 9, 1–13. <https://doi.org/10.1007/BF01969526>.
42. Iino, C., and Shimoyama, T. (2021). Impact of *Helicobacter pylori* infection on gut microbiota. *World J. Gastroenterol.* 27, 6224–6230. <https://doi.org/10.3748/wjg.v27.i37.6224>.
43. Grabrucker, S., Marizzoni, M., Silajđić, E., Lopizzo, N., Mombelli, E., Nicolas, S., Dohm-Hansen, S., Scassellati, C., Moretti, D.V., Rosa, M., et al. (2023). Microbiota from Alzheimer's patients induce deficits in cognition and hippocampal neurogenesis. *Brain* 146, awad303. <https://doi.org/10.1093/brain/awad303>.
44. Tett, A., Pasolli, E., Masetti, G., Ercolini, D., and Segata, N. (2021). Prevotella diversity, niches and interactions with the human host. *Nat. Rev. Microbiol.* 19, 585–599. <https://doi.org/10.1038/s41579-021-00559-y>.
45. Summanen, P.H., Talan, D.A., Strong, C., McTeague, M., Bennon, R., Thompson, J.E., Jr., Väisänen, M.-L., Moran, G., Winer, M., and Finegold, S.M. (1995). Bacteriology of Skin and Soft-Tissue Infections: Comparison of Infections in Intravenous Drug Users and Individuals with No History of Intravenous Drug Use. *Clin. Infect. Dis.* 20, S279–S282. https://doi.org/10.1093/clinids/20.Supplement_2.S279.
46. Civen, R., Jousimies-Somer, H., Marina, M., Borenstein, L., Shah, H., and Finegold, S.M. (1995). A Retrospective Review of Cases of Anaerobic Empyema and Update of Bacteriology. *Clin. Infect. Dis.* 20, S224–S229.
47. Socransky, S.s., Haffajee, A.d., Cugini, M.a., Smith, C., and Kent, R.L., Jr. (1998). Microbial complexes in subgingival plaque. *J. Clin. Periodontol.* 25, 134–144. <https://doi.org/10.1111/j.1600-051X.1998.tb02419.x>.
48. Kim, S.-J., Choi, E.-Y., Kim, E.G., Shin, S.-H., Lee, J.-Y., Choi, J.-I., and Choi, I.-S. (2007). Prevotella intermedia lipopolysaccharide stimulates release of tumor necrosis factor- α through mitogen-activated protein kinase signaling pathways in monocyte-derived macrophages. *FEMS Immunol. Med. Microbiol.* 51, 407–413. <https://doi.org/10.1111/j.1574-695X.2007.00318.x>.
49. Xu, P., Shao, R.R., Zhang, S., Tan, Z.W., Guo, Y.T., and He, Y. (2022). The mechanism on Prevotella melaninogenica promoting the inflammatory progression of oral lichen planus. *Clin. Exp. Immunol.* 209, 215–224. <https://doi.org/10.1093/cei/uxac054>.
50. Marietta, E.V., Murray, J.A., Luckey, D.H., Jeraldo, P.R., Lamba, A., Patel, R., Luthra, H.S., Mangalam, A., and Taneja, V. (2016). Human Gut-Derived Prevotella histiolica Suppresses Inflammatory Arthritis in Humanized Mice. *Arthritis Rheumatol.* 68, 2878–2888. <https://doi.org/10.1002/art.39785>.
51. Larsen, J.M. (2017). The immune response to Prevotella bacteria in chronic inflammatory disease. *Immunology* 151, 363–374. <https://doi.org/10.1111/imm.12760>.
52. Beydoun, M.A., Beydoun, H.A., Hossain, S., El-Hajj, Z.W., Weiss, J., and Zonderman, A.B. (2020). Clinical and Bacterial Markers of Periodontitis and Their Association with Incident All-Cause and Alzheimer's Disease Dementia in a Large National Survey. *J. Alzheimers Dis.* 75, 157–172. <https://doi.org/10.3233/JAD-200064>.
53. Ilhan, Z.E., Kaniowski, P., Tonachio, A., and Herbst-Kralovetz, M.M. (2020). Members of Prevotella Genus Distinctively Modulate Innate Immune and Barrier Functions in a Human Three-Dimensional Endometrial Epithelial Cell Model. *J. Infect. Dis.* 222, 2082–2092. <https://doi.org/10.1093/infdis/jiaa324>.
54. Mack, D.R., Michail, S., Wei, S., McDougall, L., and Hollingsworth, M.A. (1999). Probiotics inhibit enteropathogenic *E. coli* adherence in vitro by inducing intestinal mucin gene expression. *Am. J. Physiol.* 276,

- G941–G950. <https://doi.org/10.1152/ajpgi.1999.276.4.G941>.
55. Pothuraju, R., Pai, P., Chaudhary, S., Siddiqui, J.A., Cox, J.L., Kaur, S., Rachagani, S., Roy, H.K., Bouvet, M., and Batra, S.K. (2022). Depletion of transmembrane mucin 4 (Muc4) alters intestinal homeostasis in a genetically engineered mouse model of colorectal cancer. *Aging* 14, 2025–2046. <https://doi.org/10.18632/aging.203935>.
56. Seguela, L., Sarnelli, G., and Esposito, G. (2020). Leaky gut, dysbiosis, and enteric glia activation: the trilogy behind the intestinal origin of Parkinson's disease. *Neural Regen. Res.* 15, 1037–1038. <https://doi.org/10.4103/1673-5374.270308>.
57. Obrenovich, M.E.M. (2018). Leaky Gut, Leaky Brain? *Microorganisms* 6, 107. <https://doi.org/10.3390/microorganisms6040107>.
58. Mu, Q., Kirby, J., Reilly, C.M., and Luo, X.M. (2017). Leaky Gut As a Danger Signal for Autoimmune Diseases. *Front. Immunol.* 8, 598. <https://doi.org/10.3389/fimmu.2017.00598>.
59. CDC (2024). Bioterrorism and Anthrax: The Threat. Anthrax. <https://www.cdc.gov/anthrax/bioterrorism/index.html>.
60. Goya, M.E., Xue, F., Sampedro-Torres-Quevedo, C., Arnaouteli, S., Riquelme-Dominguez, L., Romanowski, A., Brydon, J., Ball, K.L., Stanley-Wall, N.R., and Doitsidou, M. (2020). Probiotic *Bacillus subtilis* Protects against α -Synuclein Aggregation in *C. elegans*. *Cell Rep.* 30, 367–380.e7. <https://doi.org/10.1016/j.celrep.2019.12.078>.
61. Haran, J.P., Bhattarai, S.K., Foley, S.E., Dutta, P., Ward, D.V., Bucci, V., and McCormick, B.A. (2019). Alzheimer's Disease Microbiome Is Associated with Dysregulation of the Anti-Inflammatory P-Glycoprotein Pathway. *mBio* 10, e00632-19. <https://doi.org/10.1128/mBio.00632-19>.
62. Kaiyrykzy, A., Kozhakhmetov, S., Babenko, D., Zholdasbekova, G., Alzhanova, D., Olzhayev, F., Baibulatova, A., Kushugulova, A.R., and Askarova, S. (2022). Study of gut microbiota alterations in Alzheimer's dementia patients from Kazakhstan. *Sci. Rep.* 12, 15115. <https://doi.org/10.1038/s41598-022-19393-0>.
63. Keshavarzian, A., Green, S.J., Engen, P.A., Voigt, R.M., Naqib, A., Forsyth, C.B., Mutlu, E., and Shannon, K.M. (2015). Colonic bacterial composition in Parkinson's disease. *Mov. Disord.* 30, 1351–1360. <https://doi.org/10.1002/mds.26307>.
64. Ragusa, M., Santagati, M., Mirabella, F., Lauletta, G., Ciriigliaro, M., Brex, D., Barbagallo, C., Domini, C.N., Gulisano, M., Barone, R., et al. (2020). Potential Associations Among Alteration of Salivary miRNAs, Saliva Microbiome Structure, and Cognitive Impairments in Autistic Children. *Int. J. Mol. Sci.* 21, 6203. <https://doi.org/10.3390/ijms21176203>.
65. Atkin, T.A., Brandon, N.J., and Kittler, J.T. (2012). Disrupted in Schizophrenia 1 forms pathological aggregates that disrupt its function in intracellular transport. *Hum. Mol. Genet.* 21, 2017–2028. <https://doi.org/10.1093/hmg/dds018>.
66. Fujita, E., Dai, H., Tanabe, Y., Zhiling, Y., Yamagata, T., Miyakawa, T., Tanokura, M., Momoi, M.Y., and Momoi, T. (2010). Autism spectrum disorder is related to endoplasmic reticulum stress induced by mutations in the synaptic cell adhesion molecule, CADM1. *Cell Death Dis.* 1, e47. <https://doi.org/10.1038/cddis.2010.23>.
67. Jaco, A.D., Lin, M.Z., Dubi, N., Comoletti, D., Miller, M.T., Camp, S., Ellisman, M., Butko, M.T., Tsien, R.Y., and Taylor, P. (2010). Neuroligin Trafficking Deficiencies Arising from Mutations in the α / β -Hydrolase Fold Protein Family. *J. Biol. Chem.* 285, 28674–28682. <https://doi.org/10.1074/jbc.M110.139519>.
68. Ješko, H., Ciešlik, M., Gromadzka, G., and Adamczyk, A. (2020). Dysfunctional proteins in neuropsychiatric disorders: From neurodegeneration to autism spectrum disorders. *Neurochem. Int.* 141, 104853. <https://doi.org/10.1016/j.neuint.2020.104853>.
69. De Angelis, M., Piccolo, M., Vannini, L., Siragusa, S., De Giacomo, A., Serrazanetti, D.I., Cristofori, F., Guerzoni, M.E., Gobetti, M., and Francavilla, R. (2013). Fecal Microbiota and Metabolome of Children with Autism and Pervasive Developmental Disorder Not Otherwise Specified. *PLoS One* 8, e76993. <https://doi.org/10.1371/journal.pone.0076993>.
70. Taniya, M.A., Chung, H.-J., Al Mamun, A., Alam, S., Aziz, M.A., Emon, N.U., Islam, M.M., Hong, S.T.S., Podder, B.R., Ara Mimi, A., et al. (2022). Role of Gut Microbiome in Autism Spectrum Disorder and Its Therapeutic Regulation. *Front. Cell. Infect. Microbiol.* 12, 915701. <https://doi.org/10.3389/fcimb.2022.915701>.
71. Gabriellaite, M., Bartell, J.A., Nørskov-Lauritsen, N., Pressler, T., Nielsen, F.C., Johansen, H.K., and Marvig, R.L. (2021). Transmission and Antibiotic Resistance of *Achromobacter* in Cystic Fibrosis. *J. Clin. Microbiol.* 59, 10. <https://doi.org/10.1128/jcm.02911-20>.
72. Veschetti, L., Boaretti, M., Saitta, G.M., Passarelli Mantovani, R., Lleò, M.M., Sandri, A., and Malerba, G. (2022). *Achromobacter* spp. prevalence and adaptation in cystic fibrosis lung infection. *Microbiol. Res.* 263, 127140. <https://doi.org/10.1016/j.micres.2022.127140>.
73. Marsac, C., Berdah, L., Thouvenin, G., Sermet-Gaudelus, I., and Corvol, H. (2021). *Achromobacter xylosoxidans* airway infection is associated with lung disease severity in children with cystic fibrosis. *ERJ Open Res.* 7, 00076-2021. <https://doi.org/10.1183/23120541.00076-2021>.
74. Bhagirath, A.Y., Li, Y., Somayajula, D., Dadashi, M., Badr, S., and Duan, K. (2016). Cystic fibrosis lung environment and *Pseudomonas aeruginosa* infection. *BMC Pulm. Med.* 16, 174. <https://doi.org/10.1186/s12890-016-0339-5>.
75. Xi, J., Ding, D., Zhu, H., Wang, R., Su, F., Wu, W., Xiao, Z., Liang, X., Zhao, Q., Hong, Z., et al. (2021). Disturbed microbial ecology in Alzheimer's disease: evidence from the gut microbiota and fecal metabolome. *BMC Microbiol.* 21, 226. <https://doi.org/10.1186/s12866-021-02286-z>.
76. Brunquell, J., Bowers, P., and Westerheide, S.D. (2014). Fluorodeoxyuridine enhances the heat shock response and decreases polyglutamine aggregation in an HSF-1-dependent manner in *Caenorhabditis elegans*. *Mech. Ageing Dev.* 141–142, 1–4. <https://doi.org/10.1016/j.mad.2014.08.002>.
77. Deng, P., Uma Nares, N., Du, Y., Lamech, L.T., Yu, J., Zhu, L.J., Pukkila-Worley, R., and Haynes, C.M. (2019). Mitochondrial UPR repression during *Pseudomonas aeruginosa* infection requires the bZIP protein ZIP-3. *Proc. Natl. Acad. Sci. USA* 116, 6146–6151. <https://doi.org/10.1073/pnas.1817259116>.
78. Haeussler, S., and Conradt, B. (2022). Methods to Study the Mitochondrial Unfolded Protein Response (UPRmt) in *Caenorhabditis elegans*. *Methods Mol. Biol.* 2378, 249–259. https://doi.org/10.1007/978-1-0716-1732-8_16.
79. Haynes, C.M., and Ron, D. (2010). The mitochondrial UPR – protecting organelle protein homeostasis. *J. Cell Sci.* 123, 3849–3855. <https://doi.org/10.1242/jcs.075119>.
80. Javed, I., Zhang, Z., Adamcik, J., Andrikopoulos, N., Li, Y., Otzen, D.E., Lin, S., Mezzenga, R., Davis, T.P., Ding, F., and Ke, P.C. (2020). Accelerated Amyloid Beta Pathogenesis by Bacterial Amyloid FapC. *Adv. Sci.* 7, 2001299. <https://doi.org/10.1002/advs.202001299>.
81. Dueholm, M.S., Otzen, D., and Nielsen, P.H. (2013). Evolutionary Insight into the Functional Amyloids of the Pseudomonads. *PLoS One* 8, e76630. <https://doi.org/10.1371/journal.pone.0076630>.
82. Isler, B., Kidd, T.J., Stewart, A.G., Harris, P., and Paterson, D.L. (2020). Achromobacter Infections and Treatment Options. *Antimicrob. Agents Chemother.* 64, e01025-20. <https://doi.org/10.1128/AAC.01025-20>.
83. Chen, S.G., Stribinskis, V., Rane, M.J., Demuth, D.R., Gozal, E., Roberts, A.M., Jagadapillai, R., Liu, R., Choe, K., Shivakumar, B., et al. (2016). Exposure to the Functional Bacterial Amyloid Protein Curli Enhances Alpha-Synuclein Aggregation in Aged Fischer 344 Rats and *Caenorhabditis elegans*. *Sci. Rep.* 6, 34477. <https://doi.org/10.1038/srep34477>.
84. Bieler, S., Estrada, L., Lagos, R., Baeza, M., Castilla, J., and Soto, C. (2005). Amyloid formation modulates the biological activity of a bacterial protein. *J. Biol. Chem.* 280, 26880–26885. <https://doi.org/10.1074/jbc.M502031200>.
85. Gidalevitz, T., Ben-Zvi, A., Ho, K.H., Brignull, H.R., and Morimoto, R.I. (2006). Progressive disruption of cellular protein folding in models of polyglutamine diseases. *Science* 311, 1471–1474. <https://doi.org/10.1126/science.1124514>.
86. Brown, G.C., Camacho, M., and Williams-Gray, C.H. (2023). The Endotoxin Hypothesis of Parkinson's Disease. *Mov. Disord.* 38, 1143–1155. <https://doi.org/10.1002/mds.29432>.
87. Brown, G.C. (2019). The endotoxin hypothesis of neurodegeneration. *J. Neuroinflammation* 16, 180. <https://doi.org/10.1186/s12974-019-1564-7>.
88. Amoureux, L., Bador, J., Fardeheb, S., Mabile, C., Couchot, C., Massip, C., Salignon, A.-L., Berlie, G., Varin, V., and Neuwirth, C. (2013). Detection of *Achromobacter xylosoxidans* in Hospital, Domestic, and Outdoor Environmental Samples and Comparison with Human Clinical Isolates. *Appl. Environ. Microbiol.* 79, 7142–7149. <https://doi.org/10.1128/AEM.02293-13>.
89. Chalhoub, H., Kampmeier, S., Kahl, B.C., and Van Bambeke, F. (2022). Role of Efflux in Antibiotic Resistance of *Achromobacter xylosoxidans* and *Achromobacter insuavis* Isolates From Patients With Cystic Fibrosis. *Front. Microbiol.* 13, 762307. <https://doi.org/10.3389/fmicb.2022.762307>.
90. Ryan, M.P., and Adley, C.C. (2014). *Ralstonia* spp.: emerging global opportunistic pathogens. *Eur. J. Clin. Microbiol. Infect.*

- Dis. 33, 291–304. <https://doi.org/10.1007/s10096-013-1975-9>.
91. Li, Y., Kumar, S., Zhang, L., Wu, H., and Wu, H. (2023). Characteristics of antibiotic resistance mechanisms and genes of *Klebsiella pneumoniae*. *Open Med.* 18, 20230707. <https://doi.org/10.1515/med-2023-0707>.
 92. Laukkanen, T., Kunutsor, S., Kauhanen, J., and Laukkanen, J.A. (2017). Sauna bathing is inversely associated with dementia and Alzheimer's disease in middle-aged Finnish men. *Age Ageing* 46, 245–249. <https://doi.org/10.1093/ageing/afw212>.
 93. Patrick, R.P., and Johnson, T.L. (2021). Sauna use as a lifestyle practice to extend healthspan. *Exp. Gerontol.* 154, 111509. <https://doi.org/10.1016/j.exger.2021.111509>.
 94. Kumsta, C., Chang, J.T., Schmalz, J., and Hansen, M. (2017). Hormetic heat stress and HSF-1 induce autophagy to improve survival and proteostasis in *C. elegans*. *Nat. Commun.* 8, 14337. <https://doi.org/10.1038/ncomms14337>.
 95. Bobkova, N.V., Garbuz, D.G., Nesterova, I., Medvinskaya, N., Samokhin, A., Alexandrova, I., Yashin, V., Karpov, V., Kukharsky, M.S., Ninkina, N.N., et al. (2014). Therapeutic Effect of Exogenous Hsp70 in Mouse Models of Alzheimer's Disease. *J. Alzheimers Dis.* 38, 425–435. <https://doi.org/10.3233/JAD-130779>.
 96. Kirkegaard, T., Gray, J., Priestman, D.A., Wallom, K.-L., Atkins, J., Olsen, O.D., Klein, A., Drndarski, S., Petersen, N.H.T., Ingemann, L., et al. (2016). Heat Shock Protein-based therapy as a potential candidate for treating sphingolipidoses. *Sci. Transl. Med.* 8, 355ra118. <https://doi.org/10.1126/scitranslmed.aad9823>.
 97. Kieran, D., Kalmar, B., Dick, J.R.T., Riddoch-Conteras, J., Burnstock, G., and Greensmith, L. (2004). Treatment with arimoclomol, a coinducer of heat shock proteins, delays disease progression in ALS mice. *Nat. Med.* 10, 402–405. <https://doi.org/10.1038/nm1021>.
 98. Yang, J., Bridges, K., Chen, K.Y., and Liu, A.Y.-C. (2008). Riluzole increases the amount of latent HSF1 for an amplified heat shock response and cytoprotection. *PLoS One* 3, e2864. <https://doi.org/10.1371/journal.pone.0002864>.
 99. Brenner, S. (1974). The genetics of *Caenorhabditis elegans*. *Genetics* 77, 71–94. <https://doi.org/10.1093/genetics/77.1.71>.
 100. Raizen, D., Song, B.-M., Trojanowski, N., and Young-Jai, Y. (2012). Methods for Measuring Pharyngeal Behaviors. In *WormBook, The C. elegans Research Community (WormBook)*.
 101. Keane, J., and Avery, L. (2003). Mechanosensory inputs influence *Caenorhabditis elegans* pharyngeal activity via ivermectin sensitivity genes. *Genetics* 164, 153–162. <https://doi.org/10.1093/genetics/164.1.153>.
 102. Walker, A.C., Bhargava, R., Vaziryan-Sani, A.S., Brust, A.S., and Czyz, D.M. (2022). Quantification of Bacterial Loads in *Caenorhabditis elegans*. *Bioprotocol* 12, e4291. <https://doi.org/10.21769/BioProtoc.4291>.
 103. Wick, R.R., Judd, L.M., Gorrie, C.L., and Holt, K.E. (2017). Unicycler: Resolving bacterial genome assemblies from short and long sequencing reads. *PLoS Comput. Biol.* 13, e1005595. <https://doi.org/10.1371/journal.pcbi.1005595>.
 104. Seemann, T. (2014). Prokka: rapid prokaryotic genome annotation. *Bioinformatics* 30, 2068–2069. <https://doi.org/10.1093/bioinformatics/btu153>.
 105. Katoh, K., Misawa, K., Kuma, K.i., and Miyata, T. (2002). MAFFT: a novel method for rapid multiple sequence alignment based on fast Fourier transform. *Nucleic Acids Res.* 30, 3059–3066. <https://doi.org/10.1093/nar/gkf436>.
 106. Stamatakis, A. (2014). RAxML version 8: a tool for phylogenetic analysis and post-analysis of large phylogenies. *Bioinformatics* 30, 1312–1313. <https://doi.org/10.1093/bioinformatics/btu033>.

STAR★METHODS

KEY RESOURCES TABLE

C. elegans strains, bacterial strains, and reagents.

REAGENT or RESOURCE	SOURCE	IDENTIFIER
Antibodies		
Living Colors JL-8 primary monoclonal antibody	Takara Bio	Cat#632381; RRID: AB_2313808
Goat anti-mouse HRP secondary antibody	Thermo Scientific	Prod#31430; RRID: AB_2548904
Bacterial and virus strains		
<i>Escherichia coli</i> OP50	Caenorhabditis Genetics Center	WB OP50; RRID: WB-STRAIN: OP50; NCBI TaxID: 637912; DC199
<i>Pseudomonas aeruginosa</i> PAO1	Shuman Lab (University of Chicago)	PAO1; DC3
<i>Acetobacteraceae</i> sp.	BEI Resources	HM-648
<i>Achromobacter xylosoxidans</i>	BEI Resources	HM-235
<i>Acidaminococcus</i> sp.	BEI Resources	HM-81
<i>Acidaminococcus</i> sp.	BEI Resources	HM-853
<i>Acinetobacter radioresistens</i>	BEI Resources	HM-107
<i>Actinomyces cardiffensis</i>	BEI Resources	HM-147
<i>Actinomyces gerencseriae</i>	BEI Resources	HM-97
<i>Actinomyces graevenitzii</i>	BEI Resources	HM-236
<i>Actinomyces israelii</i>	BEI Resources	HM-98
<i>Actinomyces johnsonii</i>	BEI Resources	HM-1070
<i>Actinomyces massiliensis</i>	BEI Resources	HM-814
<i>Actinomyces neuii</i>	BEI Resources	HM-1266
<i>Actinomyces odontolyticus</i>	BEI Resources	HM-94
<i>Actinomyces</i> sp.	BEI Resources	HM-1090
<i>Actinomyces</i> sp.	BEI Resources	HM-146
<i>Actinomyces urogenitalis</i>	BEI Resources	HM-1089
<i>Actinomyces viscosus</i>	BEI Resources	HM-238
<i>Aggregatibacter aphrophilus</i>	BEI Resources	HM-206
<i>Akkermansia</i> sp.	BEI Resources	HM-844
<i>Alloscardovia omnicolens</i>	BEI Resources	HM-1282
<i>Anaerococcus hydrogenalis</i>	BEI Resources	HM-1292
<i>Anaerococcus lactolyticus</i>	BEI Resources	HM-1034
<i>Anaerostipes</i> sp.	BEI Resources	HM-220
<i>Arcobacter butzleri</i>	BEI Resources	HM-298
<i>Arthrobacter albus</i>	BEI Resources	HM-1152
<i>Atopobium parvulum</i>	BEI Resources	HM-1035
<i>Atopobium parvulum</i>	BEI Resources	HM-1084
<i>Atopobium</i> sp.	BEI Resources	HM-839
<i>Bacteroides caccae</i>	BEI Resources	HM-728
<i>Bacteroides cellulosilyticus</i>	BEI Resources	HM-726
<i>Bacteroides dorei</i>	BEI Resources	HM-717
<i>Bacteroides eggerthii</i>	BEI Resources	HM-210
<i>Bacteroides fingoldii</i>	BEI Resources	HM-727
<i>Bacteroides fragilis</i>	BEI Resources	HM-20

(Continued on next page)

Continued

REAGENT or RESOURCE	SOURCE	IDENTIFIER
<i>Bacteroides fragilis</i>	BEI Resources	HM-709
<i>Bacteroides ovatus</i>	BEI Resources	HM-222
<i>Bacteroides salyersiae</i>	BEI Resources	HM-725
<i>Bacteroides</i> sp.	BEI Resources	HM-18
<i>Bacteroides stercoris</i>	BEI Resources	HM-1036
<i>Bacteroides vulgatus</i>	BEI Resources	HM-720
<i>Bacteroidetes</i>	BEI Resources	HM-4
<i>Bifidobacterium adolescentis</i>	BEI Resources	HM-633
<i>Bifidobacterium angulatum</i>	BEI Resources	HM-1189
<i>Bifidobacterium breve</i>	BEI Resources	HM-856
<i>Bifidobacterium longum</i>	BEI Resources	HM-846
<i>Bifidobacterium</i> sp.	BEI Resources	HM-30
<i>Campylobacter coli</i>	BEI Resources	HM-296
<i>Campylobacter upsaliensis</i>	BEI Resources	HM-297
<i>Capnocytophaga ochracea</i>	BEI Resources	HM-15
<i>Capnocytophaga</i> sp.	BEI Resources	HM-840
<i>Capnocytophaga sputigena</i>	BEI Resources	HM-1037
<i>Cardiobacterium valvarum</i>	BEI Resources	HM-477
<i>Catabacter hongkongensis</i>	BEI Resources	HM-1192
<i>Citrobacter portucalensis</i>	BEI Resources	HM-299
<i>Citrobacter</i> sp.	BEI Resources	HM-34
<i>Clostridiales</i> bacterium	BEI Resources	HM-1098
<i>Clostridiales</i> bacterium	BEI Resources	HM-793
<i>Clostridiales</i> sp.	BEI Resources	HM-1182
<i>Clostridium boltea</i>	BEI Resources	HM-318
<i>Clostridium cadaveris</i>	BEI Resources	HM-1039
<i>Clostridium cadaveris</i>	BEI Resources	HM-1041
<i>Clostridium citroniae</i>	BEI Resources	HM-315
<i>Clostridium clostridioforme</i>	BEI Resources	HM-306
<i>Clostridium difficile</i>	BEI Resources	HM-745
<i>Clostridium difficile</i>	BEI Resources	HM-746
<i>Clostridium difficile</i>	BEI Resources	HM-88
<i>Clostridium innocuum</i>	BEI Resources	HM-173
<i>Clostridium orbiscindens</i>	BEI Resources	HM-1044
<i>Clostridium orbiscindens</i>	BEI Resources	HM-303
<i>Clostridium</i> sp.	BEI Resources	HM-287
<i>Clostridium</i> sp.	BEI Resources	HM-36
<i>Clostridium symbiosum</i>	BEI Resources	HM-309
<i>Collinsella</i> sp.	BEI Resources	HM-304
<i>Coprobacillus</i> sp.	BEI Resources	HM-85
<i>Coprococcus</i> sp.	BEI Resources	HM-794
<i>Corynebacterium amycolatum</i>	BEI Resources	HM-109
<i>Corynebacterium</i> sp.	BEI Resources	HM-1295
<i>Corynebacterium</i> sp.	BEI Resources	HM-784
<i>Corynebacterium tuscaniense</i>	BEI Resources	HM-1153

(Continued on next page)

Continued

REAGENT or RESOURCE	SOURCE	IDENTIFIER
<i>Deinococcus grandis</i>	BEI Resources	HM-111
<i>Dermabacter</i> sp.	BEI Resources	HM-857
<i>Dorea formicigenerans</i>	BEI Resources	HM-300
<i>Eggerthella</i> sp.	BEI Resources	HM-1099
<i>Enterococcus faecalis</i>	BEI Resources	HM-432
<i>Enterococcus faecium</i>	BEI Resources	HM-968
<i>Erysipelotrichaceae</i> sp.	BEI Resources	HM-180
<i>Escherichia coli</i>	BEI Resources	HM-340
<i>Escherichia coli</i>	BEI Resources	HM-341
<i>Escherichia</i> sp.	BEI Resources	HM-38
<i>Eubacterium infirmum</i>	BEI Resources	HM-369
<i>Eubacterium</i> sp.	BEI Resources	HM-766
<i>Facklamia</i> sp.	BEI Resources	HM-289
<i>Faecalibacterium prausnitzii</i>	BEI Resources	HM-473
<i>Fingoldia magna</i>	BEI Resources	HM-1285
<i>Fusobacterium gonidiaformans</i>	BEI Resources	HM-1274
<i>Fusobacterium nucleatum</i>	BEI Resources	HM-75
<i>Fusobacterium nucleatum</i>	BEI Resources	HM-260
<i>Fusobacterium</i> sp.	BEI Resources	HM-871
<i>Fusobacterium ulcerans</i>	BEI Resources	HM-57
<i>Gardnerella vaginalis</i>	BEI Resources	HM-1105
<i>Gemella asaccharolytica</i>	BEI Resources	HM-1242
<i>Gemella haemolysans</i>	BEI Resources	HM-239
<i>Gemella morbillorum</i>	BEI Resources	HM-240
<i>Gemella sanguinis</i>	BEI Resources	HM-241
<i>Granulicatella adiacens</i>	BEI Resources	HM-1047
<i>Helicobacter pullorum</i>	BEI Resources	HM-124
<i>Helicobacter pylori</i>	BEI Resources	HM-273
<i>Hungatella hathewayi</i>	BEI Resources	HM-308
<i>Klebsiella oxytoca</i>	BEI Resources	HM-624
<i>Klebsiella pneumoniae</i>	BEI Resources	HM-751
<i>Klebsiella</i> sp.	BEI Resources	HM-354
<i>Klebsiella</i> sp.	BEI Resources	HM-44
<i>Lachnoanaerobaculum</i> sp.	BEI Resources	HM-780
<i>Lactobacillus oris</i>	BEI Resources	HM-560
<i>Lactobacillus crispatus</i>	BEI Resources	HM-375
<i>Lactobacillus gasseri</i>	BEI Resources	HM-399
<i>Lactobacillus gasseri</i>	BEI Resources	HM-647
<i>Lactobacillus iners</i>	BEI Resources	HM-702
<i>Lactobacillus jensenii</i>	BEI Resources	HM-646
<i>Lactobacillus johnsonii</i>	BEI Resources	HM-643
<i>Lactobacillus parafarraginis</i>	BEI Resources	HM-478
<i>Lactobacillus rhamnosus</i>	BEI Resources	HM-106
<i>Leptotrichia goodfellowii</i>	BEI Resources	HM-12
<i>Listeria monocytogenes</i>	BEI Resources	HM-1048

(Continued on next page)

Continued

REAGENT or RESOURCE	SOURCE	IDENTIFIER
<i>Mageeibacillus indolicus</i>	BEI Resources	HM-1095
<i>Megasphaera micronuciformis</i>	BEI Resources	HM-1172
<i>Microbacterium</i> sp.	BEI Resources	HM-841
<i>Micrococcus luteus</i>	BEI Resources	HM-114
<i>Mobiluncus mulieris</i>	BEI Resources	HM-125
<i>Neisseria flavescens</i>	BEI Resources	HM-115
<i>Neisseria mucosa</i>	BEI Resources	HM-242
<i>Neisseria</i> sp.	BEI Resources	HM-91
<i>Olsenella</i> sp.	BEI Resources	HM-1239
<i>Olsenella uli</i>	BEI Resources	HM-877
<i>Oribacterium sinus</i>	BEI Resources	HM-13
<i>Oscillibacter</i> sp.	BEI Resources	HM-1030
<i>Oxalobacter formigenes</i>	BEI Resources	HM-1
<i>Paenibacillus barengoltzii</i>	BEI Resources	HM-1049
<i>Paenisporosarcina</i> sp.	BEI Resources	HM-788
<i>Parabacteroides goldsteinii</i>	BEI Resources	HM-1050
<i>Parabacteroides merdae</i>	BEI Resources	HM-729
<i>Parvimonas micra</i>	BEI Resources	HM-1052
<i>Parvimonas</i> sp.	BEI Resources	HM-1253
<i>Parvimonas</i> sp.	BEI Resources	HM-207
<i>Peptoniphilus lacrimalis</i>	BEI Resources	HM-1161
<i>Peptoniphilus</i> sp.	BEI Resources	HM-825
<i>Peptoniphilus</i> sp.	BEI Resources	HM-263
<i>Peptostreptococcaceae</i> bacterium	BEI Resources	HM-483
<i>Peptostreptococcus</i> sp.	BEI Resources	HM-1051
<i>Phascolarctobacterium</i> sp.	BEI Resources	HM-179
<i>Plesiomonas</i> sp.	BEI Resources	HM-791
<i>Porphyromonas gingivalis</i>	BEI Resources	HM-1071
<i>Porphyromonas gingivalis</i>	BEI Resources	HM-1073
<i>Porphyromonas</i> sp.	BEI Resources	HM-1064
<i>Porphyromonas</i> sp.	BEI Resources	HM-781
<i>Porphyromonas uenonis</i>	BEI Resources	HM-130
<i>Prevotella amnii</i>	BEI Resources	HM-138
<i>Prevotella bivia</i>	BEI Resources	HM-1165
<i>Prevotella bivia</i>	BEI Resources	HM-1270
<i>Prevotella bivia</i>	BEI Resources	HM-1286
<i>Prevotella buccae</i>	BEI Resources	HM-45
<i>Prevotella corporis</i>	BEI Resources	HM-1294
<i>Prevotella denticola</i>	BEI Resources	HM-1173
<i>Prevotella denticola</i>	BEI Resources	HM-208
<i>Prevotella disiens</i>	BEI Resources	HM-1171
<i>Prevotella histicola</i>	BEI Resources	HM-471
<i>Prevotella melaninogenica</i>	BEI Resources	HM-80
<i>Prevotella nigrescens</i>	BEI Resources	HM-271
<i>Prevotella oralis</i>	BEI Resources	HM-1054

(Continued on next page)

Continued

REAGENT or RESOURCE	SOURCE	IDENTIFIER
<i>Prevotella oralis</i>	BEI Resources	HM-849
<i>Prevotella oris</i>	BEI Resources	HM-93
<i>Prevotella</i> sp.	BEI Resources	HM-1103
<i>Prevotella</i> sp.	BEI Resources	HM-16
<i>Prevotella</i> sp.	BEI Resources	HM-5
<i>Prevotella timonensis</i>	BEI Resources	HM-136
<i>Prevotella veroralis</i>	BEI Resources	HM-92
<i>Propionibacterium acidifaciens</i>	BEI Resources	HM-8
<i>Propionibacterium acnes</i>	BEI Resources	HM-491
<i>Propionibacterium propionicum</i>	BEI Resources	HM-209
<i>Propionibacterium</i> sp.	BEI Resources	HM-843
<i>Pseudomonas</i> sp.	BEI Resources	HM-860
<i>Psychrobacter</i> sp.	BEI Resources	HM-332
<i>Ralstonia</i> sp.	BEI Resources	HM-158
<i>Rhodococcus erythropolis</i>	BEI Resources	HM-116
<i>Rothia aeria</i>	BEI Resources	HM-818
<i>Rothia dentocariosa</i>	BEI Resources	HM-245
<i>Rothia mucilaginoso</i>	BEI Resources	HM-1055
<i>Ruminococcaceae</i> sp.	BEI Resources	HM-79
<i>Ruminococcus gnavus</i>	BEI Resources	HM-1056
<i>Ruminococcus lactaris</i>	BEI Resources	HM-1057
<i>Scardovia wiggisiae</i>	BEI Resources	HM-470
<i>Selenomonas noxia</i>	BEI Resources	HM-270
<i>Selenomonas</i> sp.	BEI Resources	HM-564
<i>Shigella</i> sp.	BEI Resources	HM-87
<i>Shuttleworthia</i> sp.	BEI Resources	HM-882
<i>Sneathia amnii</i>	BEI Resources	NR-50515
<i>Solobacterium moorei</i>	BEI Resources	HM-1058
<i>Solobacterium moorei</i>	BEI Resources	HM-1059
<i>Sporosarcina</i> sp.	BEI Resources	HM-331
<i>Staphylococcus aureus</i>	BEI Resources	HM-466
<i>Staphylococcus capitis</i>	BEI Resources	HM-117
<i>Staphylococcus caprae</i>	BEI Resources	HM-143
<i>Staphylococcus epidermidis</i>	BEI Resources	HM-140
<i>Staphylococcus haemolyticus</i>	BEI Resources	HM-1164
<i>Staphylococcus hominis</i>	BEI Resources	HM-119
<i>Staphylococcus lugdunensis</i>	BEI Resources	HM-141
<i>Staphylococcus warneri</i>	BEI Resources	HM-120
<i>Stomatobaculum longum</i>	BEI Resources	HM-480
<i>Streptococcus anginosus</i>	BEI Resources	HM-282
<i>Streptococcus cristatus</i>	BEI Resources	HM-163
<i>Streptococcus downei</i>	BEI Resources	HM-475
<i>Streptococcus gallolyticus</i>	BEI Resources	HM-272
<i>Streptococcus intermedius</i>	BEI Resources	HM-368
<i>Streptococcus mitis</i>	BEI Resources	HM-262

(Continued on next page)

Continued

REAGENT or RESOURCE	SOURCE	IDENTIFIER
<i>Streptococcus parasanguinis</i>	BEI Resources	HM-1060
<i>Streptococcus pneumoniae</i>	BEI Resources	HM-145
<i>Streptococcus salivarius</i>	BEI Resources	HM-121
<i>Streptococcus sobrinus</i>	BEI Resources	HM-1063
<i>Streptococcus</i> sp.	BEI Resources	HM-885
<i>Streptococcus vestibularis</i>	BEI Resources	HM-561
<i>Sutterella wadsworthensis</i>	BEI Resources	HM-852
<i>Tissierella bacterium</i>	BEI Resources	HM-1096
<i>Treponema denticola</i>	BEI Resources	HM-569
<i>Treponema denticola</i>	BEI Resources	HM-575
<i>Varibaculum cambriense</i>	BEI Resources	HM-1190
<i>Veillonella atypica</i>	BEI Resources	HM-1301
<i>Veillonella montpellierensis</i>	BEI Resources	HM-1157
<i>Veillonella</i> sp.	BEI Resources	HM-778
<i>Weissella cibaria</i>	BEI Resources	HM-1200

Chemicals, peptides, and recombinant proteins

Levamisole	Fisher Scientific	Cat#ICN15522805
Cholesterol	MP Biomedicals	Cat#101382
Powdered nonfat milk	Research Products International	M17200-1000
Tween 20	Fisher BioReagents	Cat#BP337-100
Trans-Blot Turbo Midi-size Transfer Stacks	BioRad	Cat#1704273
Trans-Blot Turbo Midi-size PDVF membrane	BioRad	Cat#10026933
Trans-Blot Turbo 5x transfer buffer	BioRad	Cat#10026938
Criterion XT Precast Gel	BioRad	Cat#3450124
XT 4x Sample Buffer	BioRad	Cat#1610791
20x Reducing Agent	BioRad	Cat#1610792
XT MOPS	BioRad	Cat#1610788
Clarity Western ECL	BioRad	Cat#1705061
Oxyrase	OXYRASE	Cat#OB-0100

Experimental models: organisms/strains

<i>C. elegans</i> : Strain AM738: <i>rmls297</i> [<i>vha-6p::q44::yfp</i> ; <i>rol-6(su1006)</i>]	Morimoto Lab (Northwestern University)	AM738; intestinal polyQ44
<i>C. elegans</i> : Strain 712: <i>rmls281</i> [<i>vha-6p::q33::yfp</i> ; <i>rol-6(su1006)</i>]	Morimoto Lab (Northwestern University)	AM712; intestinal polyQ33
<i>C. elegans</i> : Strain AM141: <i>rmls133[unc-54p::q40::yfp]</i>	Morimoto Lab (Northwestern University)	AM141; muscle polyQ40
<i>C. elegans</i> : Strain AM140: <i>rmls132[unc-54p::q35::yfp]</i>	Morimoto Lab (Northwestern University)	AM140; muscle polyQ35
<i>C. elegans</i> : Strain AM134: <i>rmls126[unc-54p::q0::yfp]</i>	Morimoto Lab (Northwestern University)	AM134; muscle polyQ0
<i>C. elegans</i> : Strain AM101: <i>rmls110[F25B3.3p::q40::yfp]</i>	Morimoto Lab (Northwestern University)	AM101; neuronal polyQ40
<i>C. elegans</i> : Strain AM52: <i>rmls182[F25B3.3p::q0::yfp]</i>	Morimoto Lab (Northwestern University)	AM52; neuronal polyQ0

(Continued on next page)

Continued

REAGENT or RESOURCE	SOURCE	IDENTIFIER
<i>C. elegans</i> : Strain JKM7: <i>Is[myo-3p::Signalpeptide-Abeta(1-42)::hsp-3(IRES)::wormScarlet-Abeta(1-42)::unc-54(3' UTR)+rps-0p::HygroR]</i>	Kirstein Lab (University of Bremen, Germany)	JKM7; muscle Aβ ₁₋₄₂
<i>C. elegans</i> : Strain JKM8: <i>Ex[myo-3p::wormScarlet-Abeta::unc-54(3' UTR)+rps-0p::HygroR]</i>	Kirstein Lab (University of Bremen, Germany)	JKM8, no Aβ ₁₋₄₂
<i>C. elegans</i> : Strain DDP1: <i>uonEx1[unc-54::alpha-synuclein::CFP+unc-54::alpha-synuclein::YFP(Venus)]</i>	Caenorhabditis Genetics Center	WB Strain: DDP1 WormBaseID: WBStrain00005628 This paper: α-syn ₁
<i>C. elegans</i> : Strain NL5901: <i>pkl52386[unc-54p::alphasynuclein::YFP+unc-119(+)]</i>	Caenorhabditis Genetics Center	WB Strain: NL5901 WormBase ID: WBStrain00029035 This paper: α-syn ₂
<i>C. elegans</i> : Strain N2	Caenorhabditis Genetics Center	WB Strain: N2 WormBase ID: WBStrain00000001 This paper: WT
<i>C. elegans</i> : Strain CB1301: <i>unc-54(e1301)</i>	Caenorhabditis Genetics Center	WB Strain: CB1301 WormBase ID: WBStrain00004294 This paper: <i>unc-54(ts)</i>
<i>C. elegans</i> : Strain CX51: <i>dyn-1(ky51) X.</i>	Caenorhabditis Genetics Center	WB Strain: CX51 WormBase ID: WBStrain00005217 This paper: <i>dyn-1(ts)</i>
<i>C. elegans</i> : Strain AM446: <i>rmls223[C12C8.1p::gfp; rol-6(su1006)]</i>	Morimoto Lab (Northwestern University)	AM446; <i>hsp70p::GFP</i>

Software and algorithms

GraphPad Prism v8.4.0	GraphPad Software, Inc	http://www.graphpad.com
BioRender	BioRender	www.biorender.com
RStudio	RStudio Integrated Development for R	http://www.rstudio.com/
BV-BCR	Bacterial and Viral Bioinformatics Resources Center	https://www.bv-brc.org/
Unicycler	N/A	https://doi.org/10.1371/JOURNAL.PCBI.1005595
Prokka	N/A	https://doi.org/10.1093/bioinformatics/btu153
MAFFT	N/A	https://doi.org/10.1093/nar/gkf436
RAxML	N/A	https://doi.org/10.1093/bioinformatics/btu033

Other

Thermo Scientific- Anaeropack	Fisher Scientific	Cat#23-246-376
ProSignal Blotting Film	Prometheus	Cat#30-810L

EXPERIMENTAL MODEL AND STUDY PARTICIPANT DETAILS

***C. elegans* maintenance**

C. elegans strains were maintained as previously described.⁹⁹ For experiments that generated the data represented in the heatmap (Figure 2), nematodes were kept on *E. coli* OP50 for two days at 20°C, washed three times and transferred to indicated bacteria, where they were kept at 22.5°C for three days. For all other experiments, age-synchronized nematodes were plated on indicated bacteria as L1s at 22.5°C, where they remained until the time of assay, except for the experiment in Figure S5 ("Muscle"), in which worms were cultured in temperatures indicated in the figure, and S5 ("Neuronal") in which worms were cultured at 15°C, assayed, then shifted to 25°C for 1 h prior to the motility assay. All *C. elegans* strains used in this study can be found in the [key resources table](#).

METHOD DETAILS

Bacterial culture conditions

All bacteria were cultured at 37°C. [Table S1](#) lists the growth condition for each bacteria represented in [Figure 2](#) (1–5): 1) anaerobically in re-inforced clostridial broth with Oxyrase, 2) facultative conditions (no shaking, tube filled to top) in brain heart infusion broth (BHI), 3) aerobic conditions, shaking at 220 revolutions per minute (RPM) in BHI, 4) anaerobic conditions on tryptic soy agar (TSA) supplemented with 5% defibrinated sheep's blood, 5) aerobic conditions on TSA supplemented with 5% defibrinated sheep's blood. *E. coli* OP50 controls were grown in a manner consistent with which experiment was performed. Bacteria were washed and resuspended in M9 before being seeded on NGM. All follow-up experiments were performed with bacteria grown on TSA supplemented with 5% defibrinated sheep's blood at 37°C except for the intestinal confirmation experiment of the proteotoxic bacteria ([Figure 4A](#), "Aggregates"), in which bacteria were grown according to growth condition "3" described above. Except for *Prevotella* spp. which were grown under anaerobic conditions, bacteria were grown aerobically in follow-up experiments.

Aggregate quantification

Fluorescent aggregates were quantified using Leica MZ10F Modular Stereo Microscope equipped with CoolLED pE300lite 365 dir mount STEREO with filter set ET GFP-MZ10F. Fluorescent aggregates in worms used to generate data for the heatmap ([Figure 2](#); [Table S1](#)) were manually quantified after having been cultured as indicated in "[C. elegans maintenance](#)." For all other experiments, worms were plated on indicated bacteria as L1s and fluorescent aggregates were manually quantified after four days (intestinal polyQ44) or three days (muscle polyQ35, 40) of life. Aggregates of worms that were quantified to generate the data used in the heatmap were quantified blind.

Motility assays

All motility assays were performed at room temperature, as previously described.^{16,17} In brief, the TOP assay entails sliding a worm pick made with an eyebrow hair under the mid-section of the worm and using a ticking second timer to count the number of seconds it takes for the worm to crawl off entirely. Longer TOP (seconds) indicates a more severe motility defect. TOP (seconds) of transgenic nematodes harboring tissue-specific aggregating protein was assessed on day three (muscle polyQ, muscle $A\beta_{1-42}$, *unc-54(ts)*, *dyn-1(ts)*, and respective controls) or four (intestine polyQ, neuron polyQ, muscle α -synuclein and respective controls) after plating on indicated bacteria as L1s. Worms carrying the temperature-sensitive mutation in *dyn-1(ts)* were assayed before and after a 1-h shift to the restrictive temperature (see "[C. elegans maintenance](#)" for details).

Feeding worms PFA-killed bacteria

Bacteria were cultured on TSA-blood plates under aerobic (*E. coli* OP50) or anaerobic (*P. corporis*) conditions, as described in "[bacterial culture conditions](#)." Bacterial lawns were washed and resuspended in M9 and adjusted to $OD_{600} = 2$. PFA was added at a final concentration of 0.5% and incubated at 37°C, shaking at 220 RPM for 1 h. After incubation, samples were washed four times by centrifugation at $5,000 \times g$ for 10 min and resuspension in M9. Bacterial killing was confirmed by spotting 20 μ L of each sample onto TSA-blood plates and incubating under the above-specified conditions. Dead bacterial samples were seeded onto NGM and allowed to dry overnight. Once dried, age-synchronized L1 worms expressing intestinal polyQ44 were plated onto them and maintained for four days in a 22.5°C incubator. PolyQ aggregates were quantified as described in "[aggregate quantification](#)."

Pharyngeal pumping

Pharyngeal pumping was assessed using a modified protocol from Raizen et al., 2012.¹⁰⁰ Bacteria were cultured on TSA-blood plates in anaerobic conditions and seeded as described in "[bacterial culture conditions](#)." Age-synchronized L1 N2s were plated onto NGM containing indicated bacteria and kept at 22.5°C for four days until the assay. After four days, each worm was picked onto a fresh plate of NGM seeded with the indicated bacteria and was given 10-15 min to acclimate. The number of pharyngeal pumps was counted over a 30-s period. A single pump was scored as a complete backward motion of the terminal bulb grinder.¹⁰¹ This was repeated on the same worm for a total of 10 times per worm.

Exposing worms to bacterial supernatants

Bacteria were grown on TSA-blood plates under aerobic (*E. coli* OP50, *K. pneumoniae*, *A. xylosoxidans*) or anaerobic (*P. corporis*) conditions. *E. coli* OP50 pellets and bacterial supernatants were obtained as follows: bacterial lawns were resuspended in M9, adjusted to $OD_{600} = 2$, centrifuged at $5,000 \times g$ for 15 min and sterile filtered. *E. coli* OP50 pellets were washed and resuspended in M9 (No SN) or supernatants from indicated bacteria. Suspensions were seeded onto NGM and allowed to dry overnight prior to having worms (intestinal polyQ44) plated on them. Details regarding worm handling and aggregate quantification can be found in "[aggregate quantification](#)."

Co-colonization assays

Bacteria were grown on TSA-blood plates under aerobic (*E. coli* OP50, *K. pneumoniae*) or anaerobic (*P. corporis*) conditions. Bacterial lawns were resuspended in M9 and indicated bacteria were mixed 1:1 (CFU/mL) and seeded on NGM. The seeded plates were allowed

to dry for 6–8 h in ambient conditions prior to having worms (intestinal polyQ44) plated on them. Details regarding worm handling and aggregate quantification can be found in “[aggregate quantification](#).”

Quantification of intestinal bacteria

Bacterial loads in the *C. elegans* intestine (N2, WT) were quantified as we have done previously. *C. elegans* were lysed using the BeadBug.¹⁰² Bacteria were cultured on TSA-blood plates in aerobic conditions as described in “[bacterial culture conditions](#).” Age-synchronized L1 N2s were plated onto NGM containing indicated bacteria and kept at 22.5°C for four days until the assay.

Live imaging

Nematodes expressing muscle-specific A β ₁₋₄₂ were plated as L1s on NGM containing *E. coli* OP50, *P. corporis* HM-1294, and *P. aeruginosa* PAO1 for three days were mounted on a 3% agarose pad, frozen to reduce background fluorescence, and imaged. Nematodes expressing *hsp70p::GFP* were plated as L1s onto NGM containing *E. coli* OP50 for two days, washed with M9 and transferred onto NGM containing indicated bacteria for 24 h, and were paralyzed with 2 mM levamisole, mounted on a 3% agarose pad, and imaged. Fluorescent and Nomarski images were taken using Zeiss Axio Observer 7 microscope equipped with AxioCam 503 mono camera, Solid-State Light Source Colibri 7, and a 10 \times EC Plan-Neofluar objective (0.3 NA) and were processed using ZEN Tiles & Positions Module in Zeiss ZenPro Software.

Gel electrophoresis and western blotting

Worms were prepared for gel electrophoresis and western blotting as previously described with a few modifications.¹⁶ In brief, M9 was used to lift worms from NGM which were washed until superficial bacteria was removed. Worms were plated on unseeded NGM, were allowed to dry briefly and 50 worms were picked into 10 μ L M9 with 1 mM phenylmethylsulfonyl fluoride (PMSF) in non-skirted screw-cap microcentrifuge tubes and frozen overnight or longer at -80°C . Tubes were pulse-centrifuged and three, 1.5 mm zirconium beads were added to each tube. The following two steps were repeated a minimum of two times; if large worm particulates were observed, these steps were repeated again with the entire sample set until no tubes contained worm pieces that were visible under a dissecting microscope: Samples were homogenized by placing tubes in a Bead Bug homogenizer at 280 \times 10 rates per minute (RPM) for 90 s. Tubes were cooled on ice and centrifuged for 1–2 min at a low speed to re-settle worms and worm particulates. Samples were transferred to new tubes with XT loading buffer and reducing agent. Samples were heated at 98°C for 7 min, cooled,¹⁶ and entire samples were loaded on 4–12% gradient sodium dodecyl sulfate-polyacrylamide gels (SDS-PAGE) to separate proteins through electrophoresis. Proteins were transferred onto polyvinylidene difluoride (PDVF) membrane, blocked with 5% nonfat milk powder in PBS-Tween-20 (PBST) and probed with Living Colors JL-8 monoclonal primary antibody (1:1000) for 48 h at 4°C on orbital shaker and underwent three, 5-min washes with 0.1% PBST followed by incubation 1:10,000 with goat-anti-mouse horseradish peroxidase conjugated secondary antibody for at least 2 h followed by three, 10-min washes with 0.1% PBST. Chemiluminescence was achieved by incubation with Clarity Western ECL substrate. Insoluble fractions were analyzed using ImageJ (v1.52) or ChemiDox XRS+-System with Image Lab Image Capture and Analysis Software. Western blots to obtain the insoluble fractions from worms that were used to generate the data used in the heatmap were conducted blind.

Heatmap generation

Heatmap was constructed in R-studio using the ComplexHeatmap package from the Bioconductor project. The experimental data were fed into R-studio as an organized.CSV file. The heatmap is the graphical representation of this data, clustering the bacteria by phylum.

Phylogenetic tree generation

Whole genome sequences were assembled using the Bacterial and Viral Bioinformatics Resources Center (BV-BCR) via Unicycler.¹⁰³ All genomes were annotated in BV-BRC using Prokka.¹⁰⁴ Phylogenetic analysis was conducted in BV-BRC based on concatenated alignments of 100 single-copy genes using mafft,¹⁰⁵ and the results were assessed for maximum likelihood using RAxML.¹⁰⁶ Sequences that did not have 100 complete single-copy genes due to poor sequencing quality were excluded.

QUANTIFICATION AND STATISTICAL ANALYSIS

Quantification of aggregate counts per worm in [Figure 2](#) was performed on a cohort of ten worms to corroborate the findings from the western blot analysis. In the rest of the figures, data are represented as the average number of aggregates, TOP (seconds), or otherwise specified per worm obtained from two independent experiments for a total of 60 worms ([Figures S2A–S2C](#) and [3A](#) “Aggregates”), 45–60 worms normalized to the control ([Figure 4A](#), “Aggregates”); three independent experiments for a total of 98 worms ([Figure S7](#)) or 60 worms ([Figure 5](#)) or 45 worms ([Figure 3A](#) “Motility” (polyQ44, polyQ33), [Figures 3B, 3C, and 4A](#) “Motility,” [Figure 4C](#) “Aggregates”) or 30 worms ([Figure 3A](#) “Motility” (N2), [Figures 3D, 3E, 4A, 4B, and 4C](#) “Motility,” [Figures 4D, 4E, S4B, S5, and S6](#)), or 20 worms ([Figure S1](#)); two independent experiments for a total of 20 worms ([Figure S3](#)). Data are described as statistically significant when $p < 0.05$ as determined by Student’s t-test or one-way ANOVA followed by multiple comparison Dunnett’s post-hoc test (statistical tests used are indicated in figure legends) performed using Graphpad Prism 8.4.3 or later. Degrees of significance are denoted by asterisks such that $*p < 0.05$, $**p < 0.01$, $***p < 0.001$, $****p < 0.0001$. Error bars represent standard error of the mean. The heatmap ([Figure 2](#)) is represented as data normalized to the control *E. coli* OP50.